Received: 14 May 2024 | Accepted: 1 July 2024

DOI: 10.1002/ecs2.70022

ECOSPHERE
AN ESA OPEN ACCESS JOURNAL

ARTICLE
Disease Ecology

A modified matrix model captures the population dynamics for the primary vector of Lyme disease in North America

John R. Foster[1] | **Shannon L. LaDeau**[2] | **Kelly Oggenfuss**[2] | **Richard S. Ostfeld**[2] | **Michael C. Dietze**[1]

[1]Department of Earth and Environment, Boston University, Boston, Massachusetts, USA

[2]Cary Institute of Ecosystem Studies, Millbrook, New York, USA

Correspondence
John R. Foster
Email: john.foster@usda.gov

Present addresses
John R. Foster, United States Department of Agriculture, Animal and Plant Health Inspection Service, Veterinary Services, Center for Epidemiology and Animal Health, Fort Collins, Colorado, USA; and Oak Ridge Institute for Science and Education, United States Department of Energy, Oak Ridge, Tennessee, USA.

Funding information
National Science Foundation, Grant/Award Number: 1638577

Handling Editor: Sunshine A. Van Bael

Abstract

Lyme disease, the most prevalent tick-borne disease in North America, is caused by the bacterium *Borrelia burgdorferi*, and in the eastern and central United States, it is spread to humans by the black-legged tick (*Ixodes scapularis*). Due to the complex, multiyear and multihost life cycle of this species, a matrix modeling approach is needed to effectively estimate subseasonal, multistage survival and transition dynamics in order to better understand and predict when population growth is high. Of the three questing tick life stages (larvae, nymphs, and adults), nymphs are most often associated with transmitting the bacteria to humans, and previous work suggests a mix of abiotic and biotic drivers are associated with nymph abundance. However, understanding tick population growth requires understanding mortality and transition probabilities for each stage and each stage may be individually and uniquely impacted by climate and host availability. A larval tick, for example, may experience warming temperatures differently than nymph or adults, because they are present on the landscape at different times. Here, we describe and validate a model that accounts for field sampling design and evaluates abiotic (temperature, relative humidity, precipitation) and biotic (host abundance) drivers of variation in tick population growth. To account for the drivers of subseasonal and interannual variability in demography, phenology, and population density, we built stage-structured population models that account for variability in meteorology and host population abundance throughout the full tick lifecycle. Our model is fit and validated with 11 years of tick and host data from the northeastern United States. In this context, we found that a four-stage model that includes unique transitions to and from a dormant, overwintering nymph state outperforms a model that only includes the three questing stages, and that incorporating the abundance of the predominant host species, *Peromyscus leucopus*, and weather variables improved predictions and model fit. Additionally, the model accurately predicted all three questing stages at sites different than where they were calibrated, showing that this model structure is

generally transferable. Overall, this model lays a foundation for the real-time iterative forecasting of tick populations needed to effectively protect public health.

KEYWORDS
data fusion, *Ixodes scapularis*; life cycle; matrix model; *Peromyscus leucopus*; population; prediction; survival, uncertainty

INTRODUCTION

In the United States, the total confirmed and probable cases of Lyme disease have more than doubled in the past decade (CDC, 2021). The disease is caused by the bacterium *Borrelia burgdorferi* (Stanek et al., 2012), and the increase in human incidence has been attributed, in part, to the range expansion of the principal vector of the bacteria, the black-legged tick (*Ixodes scapularis*) (Eisen & Eisen, 2018; Sonenshine, 2018).

I. scapularis has three post-egg life stages (larvae, nymphs, and adults). Larvae and nymphs require a blood meal to molt into the subsequent life stage, and adult female ticks require a blood meal to reproduce (Gray et al., 2002; Stanek et al., 2012). Ticks can be infected by the bacteria through any one of their necessary bloodmeals, but because *B. burgdorferi* is not maternally transmitted to larvae, host-seeking larvae are uninfected. Nymphs are generally considered to be the most epidemiologically important life history stage, with the seasonal peak onset of Lyme disease symptoms coinciding closely to the seasonal peak of host-seeking activity of nymphs (Mather et al., 1996; Nicholson & Mather, 1996; Pepin et al., 2012; Stafford et al., 1998). Adult *I. scapularis* can be infected with *B. burgdorferi*, but their lower abundance, autumn activity peak, and much larger size (and higher detectability) reduce their impact on pathogen transmission. In the northeastern United States, nymphs emerge from dormancy in late spring and early summer (May–June). This latent state reflects the prolonged transition as engorged larvae molt into nymphs, which extends through the autumn and winter before the nymphs seek a host the following summer (Ostfeld, 2011), at a time when human outdoor activity is also on the rise (Barbour & Fish, 1993; Lindsay et al., 1998).

Like nymphs, larvae and adults show strong seasonality in host-seeking activity. Adults are primarily active between September and January (Levi et al., 2015), and are important because they are competent vectors of *B. burgdorferi* (Piesman et al., 1991), and their survival and host-finding success influence the number of larvae in the next year (Wilson et al., 1990). Larvae are active between July and October (Lindsay et al., 1998), and while not infected with *B. burgdorferi* (Richter et al., 2012; Rollend et al., 2013), survival and infection of larvae determine the abundance of infected nymphs (Gray et al., 2002).

There have been numerous efforts to understand what drives the dynamics of *I. scapularis* nymphs (Ostfeld & Brunner, 2015). The abundance of white-footed mice (*Peromyscus leucopus*) in midsummer, which itself is associated with prior acorn abundance, predicts the abundance of infected *I. scapularis* nymphs the following spring/summer (Ostfeld et al., 1996, 2001, 2018). The positive relationship between mouse abundance and subsequent tick abundance is caused by the high permissiveness of *P. leucopus* to tick feeding (Keesing et al., 2009) and their high efficiency at transmitting *B. burgdorferi* to feeding larvae (Ostfeld et al., 2018; Schmidt & Ostfeld, 2001). The inclusion of hosts, such as mice, in models has been justified based on the important role they play in the tick life cycle more generally, and in tick-borne disease ecology specifically.

Abiotic variables, such as weather, have also been evaluated as predictors of tick abundance and activity. Increasing winter precipitation and annual precipitation are positively correlated with nymph density (Hayes et al., 2015; Jones & Kitron, 2000; Kessler et al., 2019) and Jones and Kitron (2000) demonstrated that cumulative rainfall is associated with larval abundance. Relative humidity (RH) is associated with questing activity of nymphal *I. scapularis* (Perret et al., 2004) and survival (Ginsberg et al., 2017; Piesman et al., 1991). Tick mortality increased with decreasing temperature for all life stages (Ogden et al., 2005), and spring temperature predicts nymph questing activity (Levi et al., 2015). Cumulative growing degree-days were positively correlated with tick abundance on drag cloths (Jones & Kitron, 2000; Ogden et al., 2008) and peak occurrence (Levi et al., 2015).

Understanding how climatic and biotic variables influence population dynamics is important for predicting tick populations into the future under an uncertain climate. However, few prior studies were designed to simultaneously estimate the effects of these intrinsic and extrinsic drivers across the multiple tick life stages. This is because a common challenge with stage-structured populations is that demographic rates, such as survival and fecundity, can be nonidentifiable when individuals are unmarked

(Gross et al., 2002), and each of these rates may be differentially influenced by environmental drivers. Dormancy is also a part of the tick life cycle that is difficult to observe in field data, during which survival may be differentially influenced by environmental conditions than during other life stages. New modeling approaches are needed that include modeling more than one life stage at a time, as well as including causal links of climatic variables to developmental, survival, and host processes (Kilpatrick et al., 2017; LaDeau et al., 2011; Ogden et al., 2014; Ostfeld & Brunner, 2015).

Our objective is to build models that capture key mechanisms of climate- and host-mediated influence to forecast the population dynamics of *I. scapularis* and characterize the uncertainty in predictions. Uncertainty analyses can elucidate the model's predictive capabilities and help identify and prioritize data limitations (Dietze, 2017a, 2017b). We develop such stage-structured models with the hope that they will be general and broadly applicable to understanding and predicting tick population dynamics at new locations and are potentially transferable to other tick species beyond the context of human Lyme disease risk. There is a long history in ecology of using stage-structured approaches to model a wide range of different animal and plant species, as they occupy an important middle ground between simple statistical approaches (e.g., ARIMA) and highly parameterized process-based models. Such models often provide the most parsimonious balance between specificity versus generality, while providing key insights into demographic processes. We fit and validate a stage-structured model in a specific region (Hudson Vally, NY, USA) with some of the most comprehensive field data available, with the potential for transferability in space, time, and taxonomy.

Bayesian data fusion and multimodel approaches have been used effectively to identify demographic parameters in stage-structured population models of plants (Evans et al., 2010), salmon (Michielsens et al., 2008), and ticks (Dobson et al., 2011). Here we describe a Bayesian data fusion approach for assimilating multiple sources of field data within a stage-structured matrix model to quantify demographic parameters (survival, transition, fecundity) and estimate population growth and stage-specific abundance using three comprehensive and long-term datasets from the Hudson Valley Region in New York. In addition to predictions of tick abundance, our approach supports the estimation of spatial variability in covariate effects influencing tick and rodent populations across three independent field sites, which allows us to determine environmental factors that contribute to spatial variation in abundance (Royle, 2004).

A tick spends >90% of its life in the soil or leaf-litter exposed to microclimatic conditions (Needham, 1991). We hypothesize that models that use abiotic data (daily weather) to drive the daily survival rate of each life stage will yield more accurate predictions of tick density compared with models that do not use abiotic data (H1). Transition between life stages can only occur if questing ticks successfully find a host (Gray et al., 2002; Keesing et al., 2009). Thus, we also hypothesize that models that use host abundance to drive life stage transitions will improve tick density estimates compared with models that do not (H2). Finally, we hypothesize that including a latent state of dormant nymphs to reflect the prolonged overwintering transition period from questing larvae to questing nymph will improve questing nymph predictions compared with predictions that do not model the dormant nymphs (H3).

METHODS

Site description and data collection

Three field sites were located at the Cary Institute of Ecosystem Studies (Cary) in Millbrook, New York (41.7851 N, −73.7338 W). Tick and mouse observations were collected at each site (Green, Henry, Tea); sites are more than 500 m apart. All sites are 2.25 ha and are post-agricultural oak-dominated forest stands (Ostfeld et al., 2001).

Tick and mouse observations

Tick (*I. scapularis*) abundances are derived from tick drags. A tick drag consists of pulling a 1-m^2 cotton cloth along the ground on three randomly chosen transects, for a total of 450 m^2 sampled per site. Ticks were counted and removed from the cloth every 30 m. Drags were conducted every three to four weeks starting in the spring of 1995 and continuing through the fall of 2005. Tick drags did not occur in the winter. This frequently employed collection method has been demonstrated to be an effective sampling protocol for estimating the abundance of questing ticks in many locations, including the northeastern United States (Eisen et al., 2019).

Mouse (*P. leucopus*) population monitoring occurred via mark–recapture concurrent with the tick monitoring. The trapping grid was an 11 × 11 array of Sherman live traps, with each station spaced 15 m apart, and two traps at each station. Traps were set for two consecutive nights every three to six weeks, baited with oats, and mice were marked with a numbered ear tag upon the first capture. Mouse captures did not occur over the winter. The minimum number of mice alive (MNA) for each site was

estimated directly from these data (Ostfeld et al., 2018). The three sites we chose to include in this study were the control sites of a long-term research program at Cary; mouse populations and vegetation were not manipulated at these sites. For more complete descriptions of the long-term tick and mouse monitoring at Cary, see Ostfeld et al. (2001), Schauber et al. (2005), Brunner & Ostfeld, 2008, and Ostfeld et al. (2018).

Meteorology

Meteorological data were collected through Cary's environmental monitoring program located on-site at a centralized location (the three Cary field sites used the same meteorological data). Precipitation was collected with a Belfort Instrument Universal Recording Rain Gauge Series 5-780, located 3 m above the ground. RH was collected with a Phys Chem Corp. PCRC-11 or PCRC-55 (years 1995–1997) and a Campbell Scientific HMP45C (years 1997–2005), and temperature was collected with a Campbell Scientific model 107 or 207 (years 1995–1998) and a Campbell Scientific HMP45C (years 1998–2005). See Kelly (2020) for a complete description of Cary's environmental monitoring program.

Prior distribution identification

We needed informative priors for larval and nymphs survival because, for example, larval survival rate is only directly measurable in the field by tracking the fate of individuals in a larval cohort, which requires some way of repeatedly identifying individuals in that cohort (e.g., marking). If, by contrast, we only track the total number of individuals in the nymph stage, then estimating the transition probability from larvae to nymph incorporates larval survival through host feeding and a successful transition (molting) to the nymphal stage, neither of which is directly observed. Therefore, from tick drag data alone, survival and transition are nonidentifiable.

We addressed this problem through the construction of data-constrained informative priors. Informative priors on the daily survival rate of black-legged larvae and nymphs were developed using data from the first year of a multiyear survival study conducted by Brunner et al. (2023). Briefly, *I. scapularis* ticks were placed inside soil core enclosures and exposed to field conditions at three sites distributed across the eastern United States: northern New York, southeastern New York, and eastern North Carolina. The first cores used in our analysis were deployed on May 11, 2017, and the last were retrieved on May 5, 2018; the cores were sampled intermittently between deployment and retrieval. In this time period, there were a total of 84 larval cores and 94 nymph cores deployed, with 15 unfed larvae and 7–12 unfed nymphs per core. We used the unfed ticks only (instead of fed or overwintering) as they represent ticks surviving in their current state, as opposed to molting or undergoing dormancy. Additionally, at the time this analysis was conducted, data on survival of adult ticks were not yet available, which is why we only have informative priors for larval and nymphal survival. Temperature and RH were monitored with Hygrochron DS1923 iButtons (Maxim Integrated, San Jose, CA) at each soil core (Brunner et al., 2023). The posterior parameter estimates from this submodel (described below) became the informative priors for our focal model, which is the matrix population model for tick density.

Statistical framework

Below we describe our statistical framework to generate predictions of tick population abundances, which includes the focal tick population model, and two submodels (Figure 1). We use matrix stage-transition models built around survival, transition, and fecundity rates to estimate the population density through time. We use two submodels to help infer survival and transition parameters in our focal model, including a model for building informative prior distributions for daily mean survival of larval and nymphal ticks, and a mouse population model used to estimate mouse abundance as a constraint on transition parameters.

All models were fit using Markov Chain Monte Carlo methods until convergence was reached. We determined convergence on marginal posterior distributions using the Gelman and Rubin convergence diagnostic (point scale reduction factor less than 1.1) implemented via the coda package in R v.4.0.2 (Brooks & Gelman, 1998; Gelman & Rubin, 1992; Plummer et al., 2006; R Core Team, 2020). Workflow, data cleaning, and analysis were completed in R. Bayesian submodels (prior identification and mouse population) were built in JAGS (Plummer, 2003), and the tick population models were built with NIMBLE (de Valpine et al., 2022; Valpine et al., 2017). Unless otherwise noted, 5000 random draws from the joint posterior were used for statistical analysis and out-of-sample predictions.

Informative priors for tick survival

To construct informative priors for the tick survival parameters used in the tick matrix stage-transition

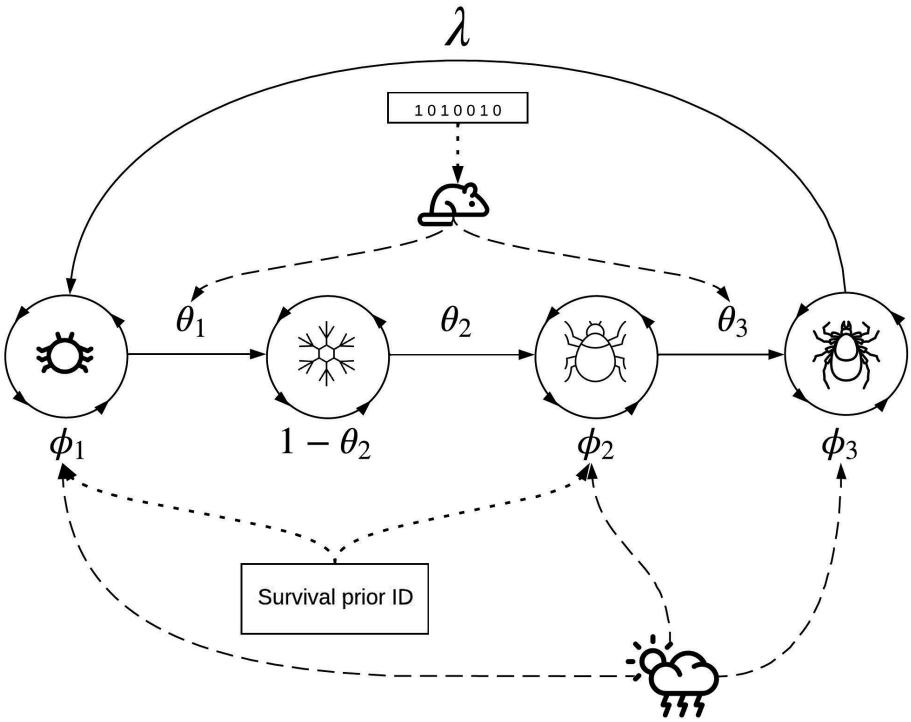

FIGURE 1 Conceptual framework. Demographic parameters (ϕ_{1-3}, θ_{1-3}, λ) map to the transition matrix (Equation 6). ϕ_{1-3} represent the daily survival rates of larvae, nymphs, and adults. θ_{1-3} represent the transition rates from larvae to dormant nymph, dormant nymph to questing nymph, and questing nymph to adult. λ is reproduction. Solid lines represent demographic processes, dashed lines represent information used as covariates (weather on survival [H1], mouse abundance on transition [H2]). Boxes and dotted lines represent the data fusion framework and location of submodels (building informed priors for larvae and nymph survival, estimating mouse abundance). The inclusion of the overwintering dormant state represents H3.

model, we used a binomial process model to estimate daily tick survival:

$$y_t \sim \text{binom}(\phi, y_0), \tag{1}$$

where y_t is the number of ticks alive at the end of the soil core experiment, y_0 is the total number of ticks that were placed in the soil, and ϕ is the cumulative survival probability over the t days ticks were in the soil. We modeled ϕ as

$$\log(\phi) = \sum_{t=1}^{d} \log(\lambda_t), \tag{2}$$

where λ_t, the daily survival probability, is connected to generalized linear model of predictors using a logit link:

$$\text{logit}(\lambda_t) = \beta X_t, \tag{3}$$

where β is a vector of regression coefficients, and $\mathbf{X_t}$ is the matrix of the average daily covariates at each site. Weather variables (aboveground daily temperature and RH) were centered so that the resulting slope coefficients represent the effect that a given weather variable has on larvae or nymph survival as the weather variable departs from its mean. Uninformative normal priors with a mean of zero were used for regression coefficients β.

Mouse population models

We examined two metrics of mouse population size as covariates in the focal tick model (Table 1). The first, the minimum number alive (MNA), was inferred from the mouse mark–recapture data directly, that is, if an individual mouse was captured on Days 1 and 3, we can infer it was alive on Day 2. The second is from a Jolly–Seber (JS) model, which was developed specifically for mark–recapture data and estimates population-level demographic parameters (Jolly, 1965; Seber, 1965). We modified the restricted dynamic occupancy model parameterization, which uses data augmentation to model the entry of not-previously-seen individuals into the population (Kéry & Schaub, 2011). Our submodel estimates the daily survival rate of mice as a function of temperature and precipitation. These abiotic factors were used primarily to constrain the overall uncertainty in mouse population estimates, because in our data fusion approach, we

TABLE 1 Models evaluated and their structures.

Model name	Model description (stages)	Covariates	Parameters constrained
Static (3)	Three-stage matrix model (questing larvae, questing nymphs, questing adults)	None	Intercepts only
Static (4)	Four-stage matrix model (questing larvae, dormant nymphs, questing nymphs, questing adults)	None	Intercepts only
MNA (4)	Four-stage matrix model	Mouse abundance (minimum number alive) from data	θ_1, θ_3
Mice Estimated (4)	Four-stage matrix model	Mouse abundance from the level-two mouse population model	θ_1, θ_3
Weather (4)	Four-stage matrix model	Daily maximum temperature, daily minimum relative humidity, daily maximum relative humidity, daily precipitation	Φ_1, Φ_2, Φ_3
Weather + Mice (4)	Four-stage matrix model	Mouse abundance from the level-two mouse population model and daily maximum temperature, daily minimum relative humidity, daily maximum relative humidity, daily precipitation	Φ_1, Φ_2, Φ_3, θ_1, θ_3

Note: Parameters constrained are from Equation (6).

assimilate the estimated mouse density with uncertainty into the focal tick model.

Because capture events were at irregular intervals, daily survival probabilities in between capture events were aggregated as follows

$$\log(\phi_d) = \sum_{t=d-\Delta d}^{d} (\log(\lambda_t)), \tag{4}$$

where ϕ_d is the probability of surviving from one capture occasion to the next. Similar to our tick focal model, we modeled daily mouse survival

$$\text{logit}(\lambda_t) = \beta_1 + \beta_2 \times \text{precipitation}_t + \beta_3 \times \text{temperature}_t, \tag{5}$$

as a logit transformed linear model of predictors. Subscript t represents each day in the time series, d represents each trapping occasion, and (Δd) represents the time elapsed since the prior trapping occasion. See Appendix S1: Section S1.1 for a complete description of this model.

Tick population models

We fit separate tick matrix stage-transition models to evaluate the influence of model structure, biotic, and abiotic variables on the accuracy and precision of modeled predictions of tick abundance. Informative prior distributions for survival (prior identification submodel, Equation 2) were used in each version of the model, and each model was fit independently to data from the three sites. Model performance was initially compared using one-step-ahead (OSA) predictions and only those that reduced OSA uncertainty are reported on.

We first built a three-stage model corresponding to the questing larvae, nymph, and adult stages (the Static model). We then added environmental covariates (temperature, RH) to the three-stage model, but neither improved model performance over the static three-stage model; the only three-stage model we report is the static version. All three-stage models had an unacceptable amount of uncertainty in out-of-sample predictions, especially for nymphs, the most epidemiologically relevant life stage.

To reduce uncertainty in nymphal predictions, we then built a four-stage model that added a dormant nymph stage. Because the four-stage model performed significantly better than the three-stage model (see *Results*), we then fit a series of five alternative four-stage models, as shown in Table 1: a Static (no covariates) model; one with daily weather variables to constrain questing tick survival; one that uses the raw mouse abundance data to constrain the transition rates from larvae to dormant nymph and from questing nymph to adult; one with the output of the estimated mouse abundance model instead of the raw mouse data; and a full model that uses both weather and estimated mouse abundance (Table 1).

We also tried to fit models with an additional dormant stage between questing adult and questing larvae (i.e., an "egg") stage but were unable to reach convergence as fecundity and adult survival became statistically nonidentifiable. We then kept the four-stage model described here because it improved nymph predictions drastically (see *Results*) and was more parsimonious than any five-stage model we could have fit.

Each transition matrix, $\mathbf{A}_t$, was estimated daily as:

$$\begin{bmatrix} \phi_1(1-\theta_1) & 0 & 0 & \lambda \\ \phi_1\theta_1 & 1-\theta_2 & 0 & 0 \\ 0 & \theta_2 & \phi_2(1-\theta_3) & 0 \\ 0 & 0 & \phi_2\theta_3 & \phi_3 \end{bmatrix}. \quad (6)$$

Parameterization of the nonzero elements can be found in Appendix S1: Section 1.2, but briefly, survival (ϕ) and transition (θ) rates are logit transformed linear models, analogous to Equation (5), and λ represents reproduction. λ, with units of larvae per adult per day, was held constant and given a prior of $N(30, 10)$ truncated at zero.

The models for survival used daily maximum temperature, daily minimum and daily maximum RH, and daily precipitation in a regularized regression framework. The survival parameters represent the probability that a questing tick remains a questing tick over a given time step, and therefore does not die and does not find a host. Specifically, Bayesian ridge regression was used to parameterize the coefficients tied to weather covariates such that $\beta_{i,w} \sim N\left(0, \gamma_\beta\right)$, where $\beta_{i,w}$ is the coefficient tied to weather covariate w of questing life stage i, and γ_β is the shrinkage penalty. This parameterization allows for collinearity in weather covariates and can improve out-of-sample prediction (Hooten & Hobbs, 2015; Tredennick et al., 2017).

The models for transition are analogous to Equation (5). Transition is defined as the probability (in a Bayesian model) that an individual moves out of the observed stage (e.g., questing larvae) and on to the next observed (e.g., questing nymph) stage, via an unobserved latent state (e.g., fed larvae). For example, there is some probability each day that a questing tick may find a host and begin the transition to a fed and molting tick. The transition rate parameters integrate over the latent state between engorgement and molting because our field data are comprised of questing ticks only.

The transition model incorporates phenology in questing behavior using cumulative growing degree-days (CGDDs) to time tick emergence (i.e., transition rate was set to zero outside of this phenological window, see Appendix S1: Equation S5). Phenological thresholds were not included in the full Bayesian model but were set a priori to occur between 400 and 2500 CGDDs for transitioning into questing nymphs, below 1000 and greater than 2500 CGDDs for adults, and between 1000 and 2500 CGDDs for transitioning into the questing larval stages (Appendix S1: Figure S1). These thresholds were based on the 11 years of tick observations in our study region. When transition was allowed to occur within these phenological windows, we tested two metrics for mouse abundance: MNA, and abundance estimated from the mark–recapture submodel. For MNA, data were treated as known, whereas we assimilated abundance estimates in an error in variables framework (Dietze, 2017a, 2017b) using the estimated mean abundance with SD (Appendix S1: Equation S6).

To compare the model with irregularly spaced observations, we permuted the matrices as follows:

$$\boldsymbol{P_d} = \boldsymbol{A_t A_{t-1} A_{t-2} \ldots A_{t-\Delta_d}}, \quad (7)$$

$$\overrightarrow{x_{d+\Delta_d}} \sim \mathrm{MVN}\left(\boldsymbol{P}_d \overrightarrow{x_d}, \Sigma\right), \quad (8)$$

where $\boldsymbol{P}_\mathrm{d}$ is the permuted transition matrix (Equation 7) that is used to calculate the expected demographic transitions between sampling occasions d. Then, the predicted latent state, $x_{d+\Delta_d}$, was drawn from the multivariate normal distribution (Equation 8) based on the expected number of ticks, $\boldsymbol{P}_d\overrightarrow{x_d}$, and a process error covariance matrix $\boldsymbol{\Sigma}$. $\boldsymbol{\Sigma}$ was parameterized as a diagonal matrix of variances, assuming that process error across life stages is uncorrelated. We attempted to fit the across-stage correlation terms but were unable to reach convergence.

Observed tick counts were assumed to be Poisson distributed, where $y_{j,d}$ is the tick count of life stage j at time d, and x is the latent tick abundance:

$$y_{j,d} \sim \mathrm{Poisson}\left(x_{j,d}\right). \quad (9)$$

Our tick field data, the number of ticks on drag cloths, integrate several ecological factors, including survival, phenology, and host abundance and diversity. Our model captures these various contributions, representing the number of individuals observed in a life stage as the balance between the number transitioning in from an early stage, the number previously in that stage that survived, and the number transitioning out to a later stage (e.g., ticks that feed and become engorged), with phenological restrictions on transition rates restricting activity to the appropriate seasons. The model defines survival as the probability ticks remain in the questing state, phenology is modeled with CGDDs, and removal by hosts is estimated in the transition model. Splitting the process in this way allows us to fit the model to the relevant

biological lifecycle of this species and makes the model generalizable because all that is needed to fit this model at a different location is counts from ticks on drag cloths.

Model assessment

The mouse population models were assessed using posterior estimates of the total predicted mouse abundance (latent abundance multiplied by capture probability) compared with observed values using R^2 and bias. Tick population models were assessed by posterior predictive checks using OSA predictions within and across sites, where the OSA predictions iteratively cycle through the time series to predict the next observation from the current latent state.

As these matrix models were fit independently at each site, the within-site predictions test goodness of fit, while the across-site predictions represent a measure of transferability and out-of-sample validation. We evaluated the OSA predictions with the continuous ranked probability score (CRPS) (Gneiting & Raftery, 2007; Simonis et al., 2021), a metric that accounts for the probabilistic nature of our predictions, penalizing models not just for mean absolute errors, but also for predictive distributions that are under- or overconfident.

A perfect forecast is defined when CRPS is equal to zero. Therefore, forecast skill increases as CRPS approaches zero; lower scores are better. Moreover, as the magnitude of observations varies considerably across life stages, we evaluated model predictions for each life stage separately.

Variance partitioning

Uncertainty in model predictions comes from four sources: (1) initial condition (IC) uncertainty, (2) parameter uncertainty, (3) driver uncertainty, and (4) process uncertainty (Dietze, 2017a, 2017b). IC, parameter, and process uncertainties were propagated by sampling the joint posterior distribution of the matrix population models. Specifically, IC uncertainty came from x (Equation 8), parameter uncertainty came from all the parameters in matrix $\mathbf{A}$ (Equation 6), and process error came from $\mathbf{\Sigma}$ (Equation 7). In terms of driver uncertainty, we treated the weather as known (without uncertainty), but incorporated uncertainty in mouse population estimates, which was derived from the posteriors of the mouse population submodel (Appendix S1: Equation S6).

To determine the contribution of each source of uncertainty, we ran OSA predictions under several scenarios, sequentially adding each source of uncertainty. The first simulation only samples from the latent state (IC) while holding parameters and drivers (estimated mouse abundance) at their posterior means and setting process error to zero. We then added parameter uncertainty, then driver uncertainty (where appropriate), and finally process uncertainty. The final scenario includes all sources of uncertainty and is the simulation that was scored with CRPS, as this scenario represents the full predictive posterior.

Population growth rate

We estimated the growth rate for each sampling season, represented by the first tick drag to the last tick drag each calendar year. Each stochastic population growth rate simulation used 2000 random draws from the joint posterior. Stochastic population growth rates were determined by sequences of the daily transition matrices $\mathbf{A}$, under a mover-advancer model in which the probability of advancing to the next environment is equal to one (Caswell, 2000).

RESULTS

Prior identification

Nymphs had a higher monthly survival rate than larvae by approximately 5% (mean across the three models was 0.509–0.517 for nymphs and 0.453–0.48 for larvae). Covariate slope parameters overlapped with zero but were consistent with higher climate sensitivity among nymphs, which responded positively to humidity and negatively to temperature, while larvae responded positively to temperature and were insensitive to humidity (Figure 2).

Mouse population models

Mean monthly survival rates of mice were similar at the three Cary sites, estimated at 0.815, 0.813, and 0.806 at Green, Henry, and Tea, respectively. Survival was negatively associated with above-average daily precipitation and temperature, with temperature having a stronger effect (median range across sites −0.058 to −0.044) than precipitation (median range across sites −0.018 to −0.015) (Appendix S1: Figure S2).

The mouse population model was fit to estimate the true abundance of mice at each field site, where these estimates were used as inputs to the focal tick population model. We evaluated the effectiveness of the mouse model by performing OSA predictions. R^2 values ranged from 0.74 to 0.77 across the three sites (Figure 3). On average,

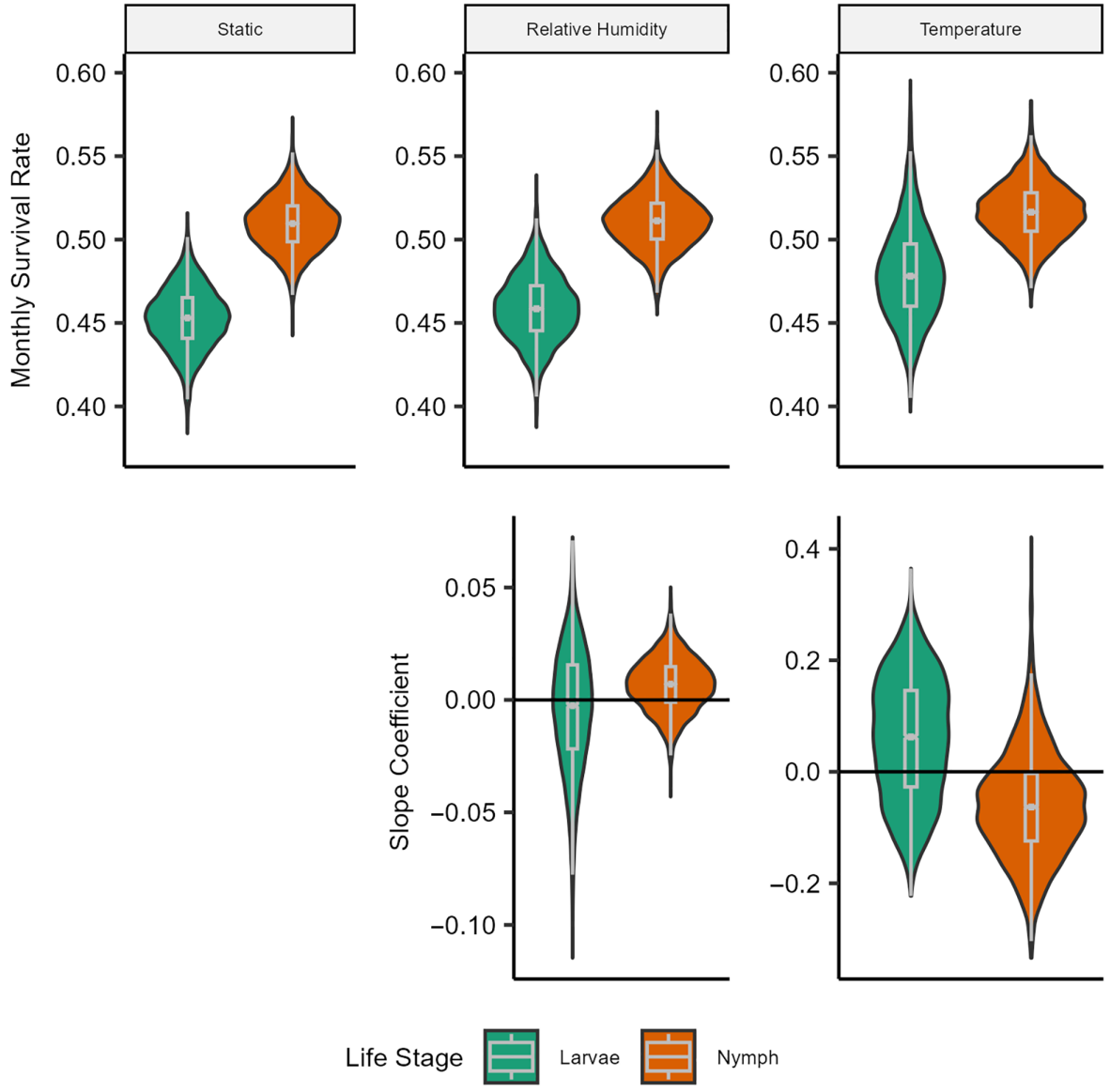

FIGURE 2 Posterior distributions from the prior identification survival models. The Static model is the intercept-only model. The covariates considered were daily relative humidity and daily temperature. The top row is the intercepts, and the bottom row is the effect of each weather variable. Violin and box plots were drawn from 5000 random samples from the posterior.

the model slightly underpredicts by roughly 6 (11.8% mean percentage error [MPE]), 3 (8.3% MPE), and 5 (11.6% MPE) mice/2.25 ha at Green, Henry, and Tea, respectively.

Tick population models

For the focal tick population models, we structure the results by hypothesis. Within each section, we first describe the predictive capacity of the models that include covariates associated with each hypothesis; models that include weather for H1, models that include mouse abundance for H2, and models that have the overwintering nymph stage for H3. After describing predictive capacity, we describe the parameters associated with each hypothesis; how weather changes the base rate of survival and the monthly rate of survival across sites and models for H1, how mouse abundance changes the base rate of transition and the monthly rate of transition across sites and models for H2, and variance partitioning in H3. We end with a description of predicted fecundity and the results of the population growth rate analysis.

The effect of daily weather (H1)

We evaluated six models with out-of-sample predictions, which means if all models were equally as predictive, we

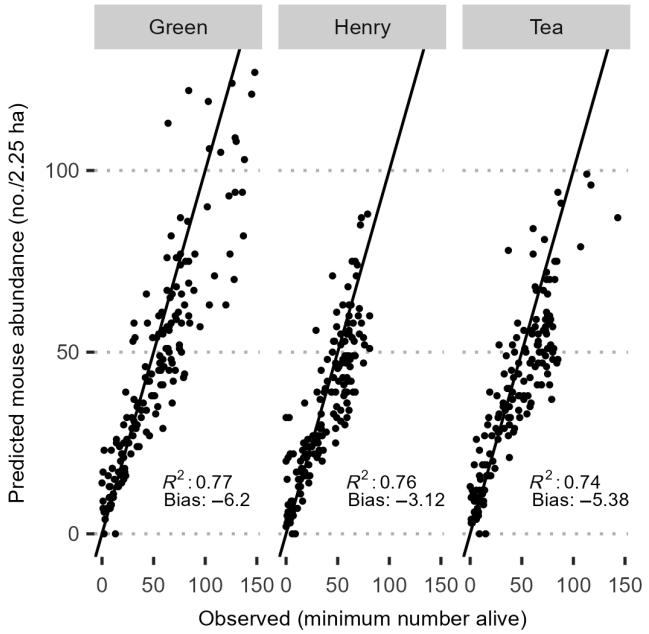

FIGURE 3 Model accuracy (the median prediction) with observation error compared with observed mice at each trapping occasion. The three sites are displayed independently. R^2 values are calculated relative to the one-to-one line. Bias represents the average number of mice underestimated per plot per trapping occasion.

would expect, on average, that each model would make the best out-of-sample prediction one-sixth (16.7%) of the time (Figure 4). For questing larvae, the Weather (4) model was the most predictive 28% of the time, and the Weather and Mice (4) model was most predictive 48% of the time according to the CRPS. For predictions outside of the larval questing season (prediction when there were zero larvae on drag cloths), the Weather (4) model was most predictive 37% of the time and the Weather and Mice (4) model was most predictive 61% of the time (Figure 4).

For questing nymphs, the Weather (4) model was the most predictive according to the CRPS 9% of the time, while the Weather and Mice (4) model was the most skillful 42% of the time. For predictions outside the nymph questing window, the Weather (4) model was most skillful 80% of the time, while the Weather and Mice (4) model was most skillful 18% of the time (Figure 4).

For questing adults, the Weather (4) model was the most predictive according to the CRPS 18% of the time, while the Weather and Mice (4) model was the most skillful 15% of the time. For predictions outside the adult questing window, the Weather (4) model was most skillful 9% of the time, while the Weather and Mice (4) model was most skillful 21% of the time (Figure 4).

The slope parameters tied to weather covariates represent the magnitude and direction of the effect that daily weather has on mean survival rate, and the intercept term in the survival equations represents the mean survival rate for each life stage. We present survival as monthly rates for easier comparison.

Daily precipitation affected larval survival the most out of the four weather variables considered (Figure 5), with a median estimate of 4.06 (90% CI: 2.08–5.97) at Green under the Weather and Mice (4) model, meaning that even a one SD increase in daily precipitation increases the odds ratio of daily larval survival by 58. At Henry, this odds ratio was 14.6, and at Tea, it was 10.31. The effect of maximum RH on larval survival was not different from zero for all sites. The effect of minimum RH on larval survival was positive and similarly estimated at Green and Tea (Figure 5). For example, at Green, the median effect of daily minimum RH was 1.27 (90% CI: 0.30–2.21), which decreases the odds ratio of larval survival by 3.6 (and by 3.8 at Tea) with a one SD increase in daily minimum RH. Daily maximum temperature did not have a significant effect on larval survival.

For nymphs, daily maximum RH had the largest effect on nymph survival of the four weather variables considered, where increasing daily maximum RH decreased survival at two of the three sites. The effect was largest at Green, with a median estimate of −1.72 (90% CI −2.28 to −0.78), followed by Tea with a median of −1.08 (90% CI −1.63 to 0.09), while the survival of nymphs at Henry was not influenced by daily maximum RH with median estimate of −0.1 (90% CI −0.71 to 0.46). This translates to decreasing the odds ratio of survival by 5.58, 2.94, and 1.11 at Green, Tea, and Henry, respectively, with a one SD increase in daily maximum RH.

Daily precipitation also had an appreciable effect on nymph survival. All sites predicted a positive influence of daily precipitation on nymph survival. The largest effect for the Weather and Mice (4) model was at Tea, with a median of 0.72 (90% CI: −0.28 to 2.45), followed by Henry with a median effect of 0.55 (90% CI −0.16 to 1.52). Nymph survival at Green was not affected by daily precipitation (Appendix S1: Table S1). All else being equal, a one SD increase in daily precipitation increases the odds ratio of daily nymph survival at Tea by 2.05, and at Henry by 1.74.

For adults, daily maximum temperature had the largest effect on adult survival of the four weather variables considered, where two of the three sites predicted a positive effect, and one a negative effect. For the sites with a predicted positive effect of daily maximum temperature on adult survival, the largest effect was at Green with a median of 3.15 (90% CI: 0.94–5.58), followed by Henry with a median of 3.0 (90% CI −0.17 to 6.06). All else

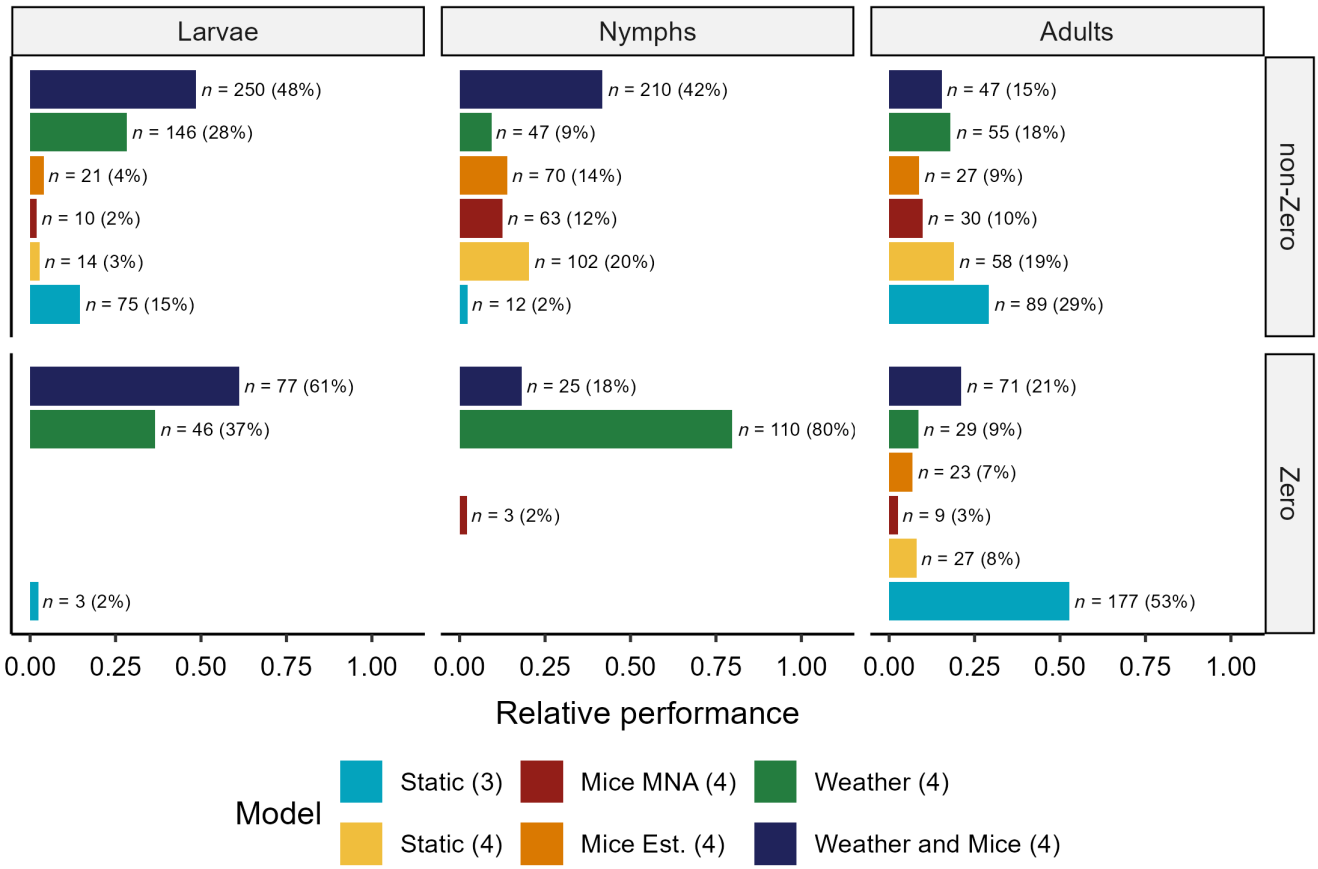

FIGURE 4 The relative performance of each model at predicting nonzero and zero observations for each life stage. Nonzero observations are during each life stage's questing period, and zero observations are during each life stage's dormancy period. *n* is the number of times a specific model had the best continuous ranked probability score; percent values are how often a specific model was most skillful relative to others. If all models were equally skillful, then the null expectation is that each model would be best one-sixth (~17%) of the time.

equal, a one SD increase in daily maximum temperature increased the odds ratio of adult survival by 23.3 at Green and by 20.1 at Henry. At Tea, there was a predicted negative influence of daily maximum temperature at Tea, with a median effect of −0.99 (90% CI −1.99 to 0.06), which equates to a decrease in the odds ratio of survival by 2.68, with a one SD increase in daily maximum temperature (Figure 5).

Survival intercepts

All predicted monthly survival estimates are reported in Appendix S1: Table S1, but there are few patterns we would like to highlight here. Under the Weather and Mice (4) model, all three sites showed similar patterns in median monthly survival across life stages, where adults survived at a higher rate than nymphs, and nymphs survived at a higher rate than larvae. For example, at Green, the median predicted monthly survival rate was 0.92 (90% CI 0.67–0.98) for adults, 0.52 (90% CI 0.49–0.54) for nymphs, and 0.45 (90% CI 0.42–0.48) for larvae. The survival estimates from the Weather (4) model were nearly identical.

For the Mice Est. (4), Mice MNA (4), and Static (4) models, the pattern of high to low survival rates in order from adult–nymph–larvae held at Green and Henry, but not at Tea. For example, at Tea under the Static (4) model, the predicted monthly survival rate was 0.37 (90% CI 0.23–0.56) for adults, 0.48 (90% CI 0.46–0.50) for nymphs, and 0.43 (90% CI 0.40–0.46) for larvae. The survival estimates from the Mice Est. (4) and Mice MNA (4) models were like that of the Static (4) model.

Estimated adult survival was less precise and more variable than for nymphs and larvae across models and sites. At Green, the median adult monthly survival rate was estimated between 0.68 and 0.92 with the Static (4) and Weather (4) models, respectively. At Henry, the range in median adult survival was between 0.76 and 0.86 with the Weather (4) and Static (3) models, respectively. The range in median adult monthly survival at Tea was between 0.37 and 0.89 with the Static (4) and

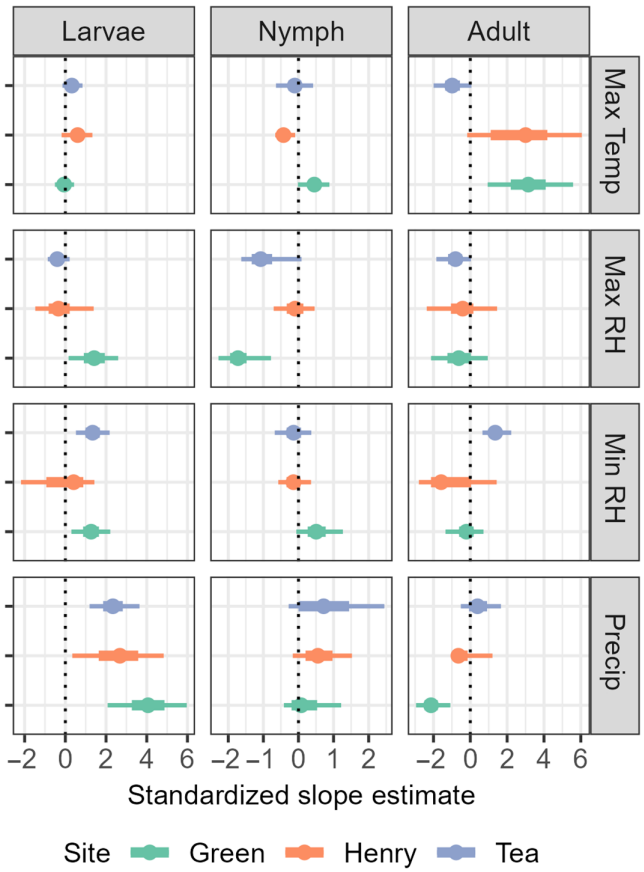

FIGURE 5 Standardized slope estimates for the effect of a given weather variable on the daily survival of a given life stage from the Weather and Mice (4) model. The width of the narrow whiskers represents the 90% CI, wide whiskers are the 50% CI, and points are the median. precip, precipitation; RH, relative humidity; Temp, temperature.

Weather (4) models, respectively. The Static (4) model had the largest range in median adult monthly survival, ranging between 0.37 at Tea and 0.82 at Henry. The Static (3) model had the smallest range across sites, where Green's median adult monthly survival was 0.77 while Henry and Tea were both estimated at 0.86 (Appendix S1: Table S1). The posterior SD for median monthly survival was, at a minimum, 2.4 times greater for adults than the other two stages. For example, at most precise estimate for mean adult survival had a SD of 0.052 at Henry under the Static (3) model, while the least precise estimate for the other two stages was for larvae at Henry under the Mice Est. (4) model with a posterior SD of 0.022.

The effect of mouse abundance (H2)

As with H1, here we describe the performance of the models that include mice relative to the null expectation that if all models were equally predictive, each would make the best OSA prediction 16.7% of the time. For questing larvae, the Mice MNA (4) model made the best OOS predictions 2% of time, the Mice Est. (4) model was best 4% of the time, and the Weather and Mice (4) model was most skillful 48% of the time. For predictions outside of the larval questing season, the Weather and Mice (4) model was most skillful 61% of the time while the Mice Est. (4) and Mice MNA (4) models were never the most skillful.

For questing nymphs, the Mice MNA (4) model was the most skillful 12% of the time, Mice Est. (4) was most skillful 14% of the time, and the Weather and Mice (4) model was the most skillful 42% of the time. For predictions when there were zero nymphs on drag cloths, the Mice MNA. (4) model was the most skillful 2% of the time, and the Weather and Mice (4) model was the most skillful 18% of the time. The Mice Est. (4) model was never the most skillful for nonquesting nymphs.

For questing adults, the Mice MNA. (4) model was most skillful for 10% of OSA predictions, the Mice Est. (4) was mode skillful for 9% of predictions, and the Weather and Mice (4) model was most skillful 15% of the time. For nonquesting adults, the Mice MNA (4) model was the most skillful 3% of the time, Mice Est. (4) 7% of the time, and the Weather and Mice (4) model 21% of the time.

The effect of mouse abundance on the daily transition rate from larva-to-nymph (L-N) was mostly consistent across sites and model formulations, where the effect was either not different from zero or mice slightly reduced the transition rate. For example, the Weather and Mice (4) model predicted no effect of mice on the L-N transition at all sites. The Mice Est. (4) model predicted a null effect at Henry and Tea, and a slight negative effect at Green, with a median estimated effect of −0.5 (90% CI −1.19–0.26). The Mice MNA (4) model had the largest range in predictions of the effect of mice on the L-N transition across sites, where there was a null effect at Tea, a slightly negative effect at Henry with a median of −0.38 (90% CI −0.91–0.16), and more pronounced effect at Green with a median of −0.91 (90% CI −1.63– −0.11); all else equal, that equates to decreasing the odds ratio of transition by 2.48 with a one SD increase in mouse abundance.

The effect of mouse abundance on the nymph-to-adult (N-A) transition was more pronounced and variable across sites and models. For the Weather and Mice (4) model, there was no predicted effect at Green and Henry, but a positive one at Tea with a median expectation of 1.42 (90% CI 0.99–0.93). The Mice Est. (4) model predicted a null effect of mice on the N-A transition at Green, and a positive effect at Henry (median of 0.55, 90% CI 0.20–0.86) and

Tea (median of 1.68, 90% CI 1.21–2.17). The Mice MNA (4) model predicted a positive effect at all sites, with Green at a median of 0.25 (90% CI −0.37–0.75), Henry at a median of 0.62 (90% CI 0.27–0.97), and Tea at a median of 1.03 (90% CI 0.80–1.34); all else equal that equates to an increase in the odds ratio of transitioning from a nymph to an adult by 2.8 with a one SD increase in mouse abundance.

Transition

Transition model intercepts represent the base rate of daily transition: we converted them to monthly rates for ease of interpretation. The monthly larvae-to-nymph (L-N) transition rate was low, with median estimates ranging from 0.002 to 0.03 for the Static (4) and Static (3) models, respectively. Furthermore, the four-stage models had very precise estimates for this parameter compared with the Static (3) model. For example, the 90% CI width at Tea for the Static (3) model was 0.01–0.061, while the largest CI interval of the four-stage models was at Tea under the Weather (4) model between 0.008 and 0.022 (Appendix S1: Figure S3).

The base monthly rate for the nymph-to-adult (N-A) transition varied across sites, and, while low, was sometimes as much as 16 times greater than the L-A transition. For example, at Tea, under the Static (4) model, the monthly N-A transition rate was estimated at 0.097 (90% CI: 0.051–0.163), whereas the L-A transition was estimated at 0.006 (90% CI: 0.003–0.01) (Appendix S1: Figure S3).

The effect of including a dormant stage (H3)

The only model that did not include the dormant nymph stage was the Static (3) model, so here we describe how predictive this model was, with the null expectation that if all models were equally predictive, then the Static (3) model would make the most skillful predictions 16.7% of the time. The Static (3) model was the most skillful for 15% and 2% of OOS predictions for questing and nonquesting larvae, respectively. It was the most skillful for 2% and 0% of OOS predictions for questing and nonquesting nymphs, respectively. Finally, the Static (3) model was the most skillful for 29% and 53% of OOS predictions for questing and nonquesting adults, respectively.

Model structural error (also referred to as process error), quantified by the variance terms in $\boldsymbol{\Sigma}$ (Equation 8), was reduced from the three-stage model to the four-stage models that included weather for larvae, to all four-stage models for nymphs, and was unchanged for adults (Figure 6).

For larvae, the addition of the dormant nymph stage only lowered process error when weather was also included. For example, process error for larvae, with units of ticks per 450 m^2 per day, under the three-stage model had a median of 17.32 (90% CI: 15.72–19.21), 11.09 (90% CI: 9.62–12.91), and 7.11 (90% CI: 6.07–8.26) at Green, Henry and Tea, respectively. Under the Weather (4) model, process error was reduced to 6.41 (90% CI: 5.69–7.29), 9.91 (90% CI: 8.38–13.3), and 6.09 (90% CI: 5.49–6.79) at Green, Henry, and Tea, respectively (Figure 6).

For nymphs, regardless of site or covariate inclusion, the addition of the dormant nymph stage reduced process error from the three-stage model to the four-stage models at all sites. For example, the Static (3) model at Green estimated process error at a median of 3.94 (90% CI: 3.62–4.31), whereas all other models at that site had a nearly 10-fold decrease in error with the lowest model estimate of process error under the Weather and Mice (4) model at a median of 0.43 (90% CI: 0.28–0.69) (Figure 6). This is apparent in the OSA simulations, where forecast uncertainty under the Static (3) model is greatly inflated compared with models with the dormant stage included (Figure 7).

Variance partitioning

We partitioned the forecast variance for each model and each life stage into the component parts that make up the total forecast uncertainty (ICs, parameter, driver, and process error). Here, we focus on the comparison of the Static (3) model to the Weather and Mice (4) model, because Weather and Mice (4) model was the most skillful at predicting questing nymphs.

The magnitude of total forecast variance throughout a given year was lowest during the inactive period for each life stage and increased substantially during the questing period. For example, larvae forecast variance peaked in July–September, nymph forecast variance peaked in May–June, and adult forecast variance peaked in October (Figure 8). This general pattern was evident in the Static (3) and Weather and Mice (4) models. The magnitude, however, was different. On average, across all OSA forecasts during the questing periods for each life stage (defined by CGDD, see *Methods*), total forecast variance was reduced by a factor of 10 for larvae, 45 for nymphs, and 2.3 for adults from the Static (3) model to the Weather and Mice (4) model.

The composition of error in OSA predictions was primarily composed of process error during the nonquesting

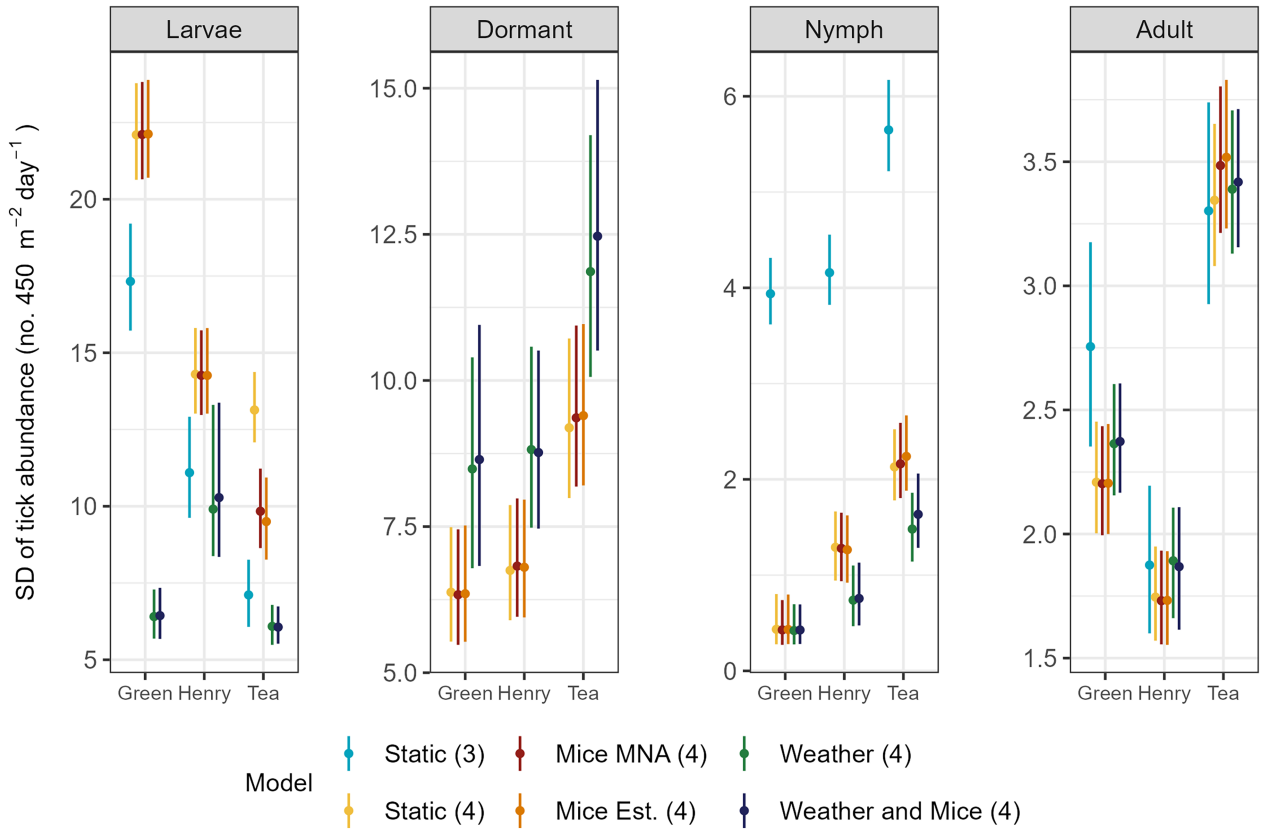

FIGURE 6 Process error distributions, represented as SDs. Facets are each life stage in the stage-structured matrix; the *x*-axis is the site a specific model (color) was calibrated. Whiskers are the 90% credible interval of the posterior, and points are the median value of process error. Note the varying *y*-axis for each facet, showing that larvae have far more process error than adults. The dormant stage was not modeled in the Static (3) model.

periods throughout the year for each life stage. It was during the questing periods that the error composition changed, where the dominant source of uncertainty shifted from being primarily process error to primarily IC error. This was particularly evident for nymphs (Figure 8). On average, across all OSA predictions during the questing period, initial condition uncertainty contributed to 2% of the overall predictive error for nymphs under the Static (3) model versus 64% under the Weather and Mice (4) model. For the other sources of uncertainty, the relative contribution to predictive error for questing nymphs was 1.4% versus 16% for parameter uncertainty, 0% versus 3% for driver uncertainty, and 96.6% versus 17% for process uncertainty.

Fecundity

We estimated variable fecundity rates among models and across sites (Appendix S1: Figure S4). For example, the Mice MNA (4) model estimated a median fecundity rate (larvae per adult per day) of 0.88 (90% CI: 0.06–5.04) at Green, 23.55 (90%: CI 17.67–31.27) at Tea, and 32.15 (90% CI: 24.45–41.49) at Henry. In general, the models that use weather to drive tick survival predict a higher reproductive rate than other model formulations. For example, the Weather and Mice (4) model estimated a reproductive rate of 41.60 (90% CI: 30.49–54.76) at Green, 44.48 (90% CI: 33.79–57.35) at Tea, and 54.44 (90% CI: 34.45–72.00) at Henry. All models updated from the prior (Appendix S1: Figure S4).

Population growth rate

Estimates of population growth rates were similar across all models and there was significant interannual variation (Figure 9). Over the 11 years of the study, population growth tended to increase across all three sites. Specifically, the tick population grew (estimated by median population growth rate) in 1999–2000, and between 2002 and 2004. The three sites show similar annual trends in growth rate, except for years 1999 and 2005. In 1999, Green and Tea have growing tick

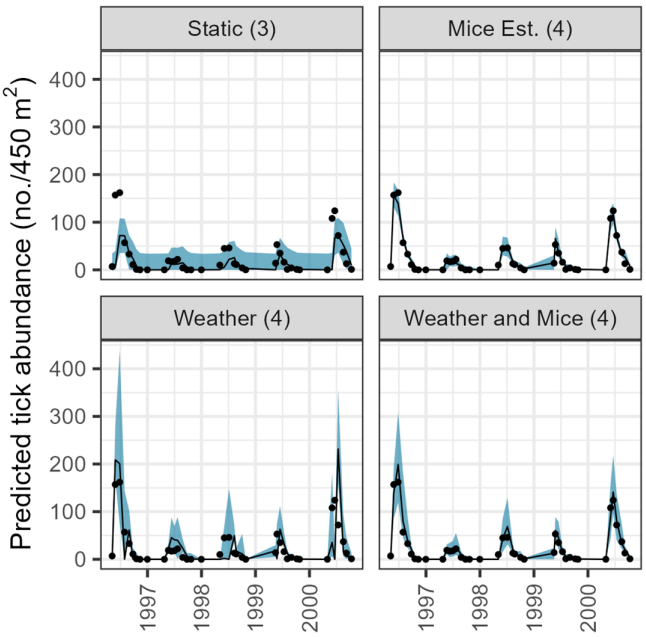

FIGURE 7 One-step ahead predictions from an across-site simulation for nymphs. The model was calibrated at Henry and simulated at Tea. Study duration was 11 years but showing 1996–2000 because peak nymphal observations were in 1996 and 2000 at Tea. Models not displayed (Static (4) and Mice MNA (4)) were excluded because they have very similar predictions to the Mice Est. (4) model. Solid points are observed values, envelope is the 95% predictive interval, and solid line is the median prediction.

populations while Henry is declining, and in 2005, Green and Tea have declining tick populations while Henry is growing. Elasticity analysis of the periodic matrix products showed that nymph and adult survival had the largest effect on population growth rate (Appendix S1: Figure S6).

DISCUSSION

This study addresses a growing need for predictive understanding of how tick populations will respond to ongoing environmental change across their complex lifecycle. Here we developed a stage-structured matrix model that estimates independent abiotic and biotic driver effects at each stage of the complex tick life history and generated a skillful predictive framework. Importantly, this framework incorporated the fusion of experimental and observational field data and uncertainty propagation across the full life cycle. Below we interpret our results considering three hypotheses concerning the importance of daily weather (H1), of the abundance of mouse hosts (H2), and of incorporating a dormant nymph stage in the modeled lifecycle structure (H3).

The effect of daily weather (H1)

We found that precipitation, temperature, and maximum humidity play critical but stage-specific roles in defining tick survival. Larval survival increased the most with increasing precipitation. By contrast, nymph survival decreased the most with increasing RH. Finally, adults were most sensitive to daily maximum temperature. The differential effect of temperature on adults (increasing survival rate) and juvenile ticks (no effect) aligns with the current understanding of tick biology. It is generally thought that a longer warm season provides fall- and spring-active adults with more chances to find a host before depleting resources and dying (Brunner et al., 2023). Larvae and nymphs quest during the warm season, when moisture is more likely to be a limiting driver than temperature (Brunner et al., 2023).

Our results are consistent with prior studies showing larval survival declines with RH (Ginsberg et al., 2014, 2017) and that average RH is not a significant predictor of nymphal abundance (Berger et al., 2014). However, our results contrast with Ginsberg et al. (2014), which showed that high RH increases nymph survival. This could be due to the discrepancy between monitoring ticks from the field as we did and monitoring ticks in the laboratory. Additionally, our model also uses precipitation as a daily driver of survival, and nymphs were estimated to have a positive association with precipitation (Figure 5). The precipitation effect could thus be overpowering the effect of RH, as days with precipitation will have a low risk of desiccation (cloudy, high RH, etc.). Also, ticks in different field locations are likely to experience different microclimate conditions, especially with respect to RH (Van Gestel et al., 2022). These ticks will, however, experience similar precipitation, and precipitation is more likely to be well represented by a central site measurement at the scale of this study. Nonetheless, our findings are consistent with prior studies in showing that tick survival is sensitive to moisture stress.

The effects of weather described above are in the context of changing the base survival rate of ticks. As such, our results agree with Brunner et al. (2012) on density-independent mortality rates, with estimated monthly survival rates between 0.4–0.45 and 0.48–0.52 for questing larvae and nymphs.

The effect of mouse abundance (H2)

We quantified the role of mice in constraining the transitions from larva to nymph and nymph to adult. The model with both weather and mice was the most skillful at predicting questing nymphs. This concurs with

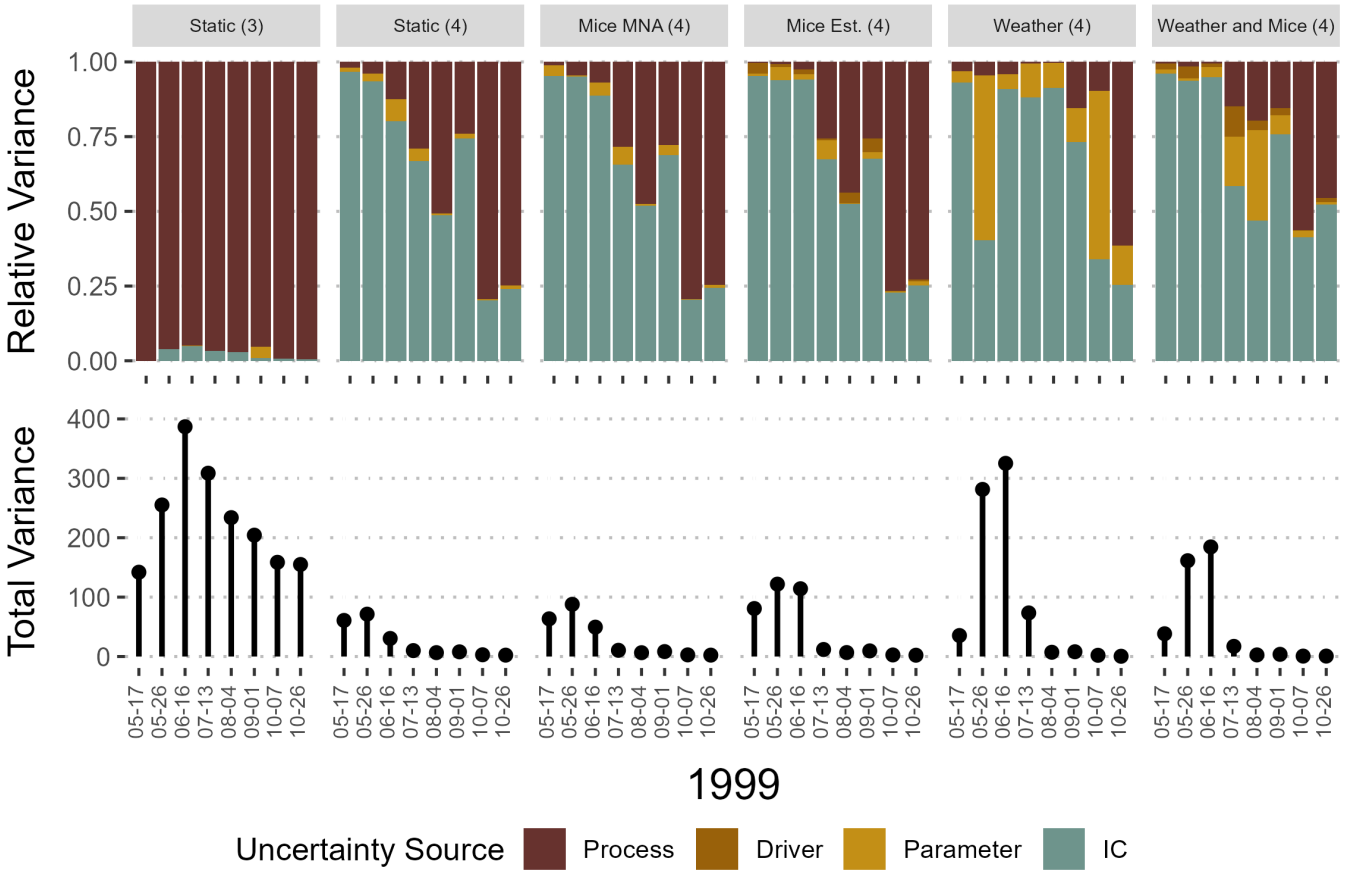

FIGURE 8 Variance partitioning for nymph predictions at Tea in 1999. The top row shows the relative proportion of the total variance that is made up of either process error (model structural uncertainty), driver error (from the mouse population model, only present in Mice Est. (4) and Weather and Mice (4) models), parameter uncertainty (from parameter distributions), and initial condition uncertainty (errors in the latent state). The bottom row shows the total amount of variance in the prediction.

previous studies that show mice play a crucial role in the ecology of *I. scapularis* in the northeast (Ostfeld et al., 2001, 2006). The ecological significance in our model comes from the idea that as nymphs emerge from dormancy as a single cohort, access to mice reduces the numbers of questing individuals (Ostfeld et al., 2018) and successful host feeding causes increased tick abundance in subsequent states (Ostfeld et al., 1996, 2001, 2018). If the concurrent mouse population acts as a removal mechanism for questing nymphal ticks, the impact of host abundance was less evident in the larva-to-nymph transition, most likely because the removal of larvae by hosts does not saturate as host density increases (Levi et al., 2016).

Additionally, mice may be relatively more important than weather in improving predictions at the transition because seasonality is more than daily weather (e.g., absence of below freezing days, daylight length, etc.), and seasonal mouse population dynamics are regulated, in part, by winter temperatures and acorn abundance (Merritt et al., 2001; Wang et al., 2009). This suggests that while mice are directly responsible for the number of ticks that feed in one stage and quest in the next, they also represent another measure of seasonality that further helps constrain OSA predictions. This explains the tendency of the Weather (4) model to overestimate nymphal abundance, as the most prominent effect of mice was on the nymph to adult transition (removing nymphs).

The effect of including a dormant stage (H3)

Including the dormant stage in the matrix between questing larvae and questing nymphs dramatically improved the predictability of nymphs (Figures 4 and 7), the life stage most responsible for Lyme disease cases in humans.

Nymphs have a longer dormancy period than other stages, which lasts through the winter (Levi et al., 2015). The addition of the latent state to the model accounts for this period when no transition occurs (transition in

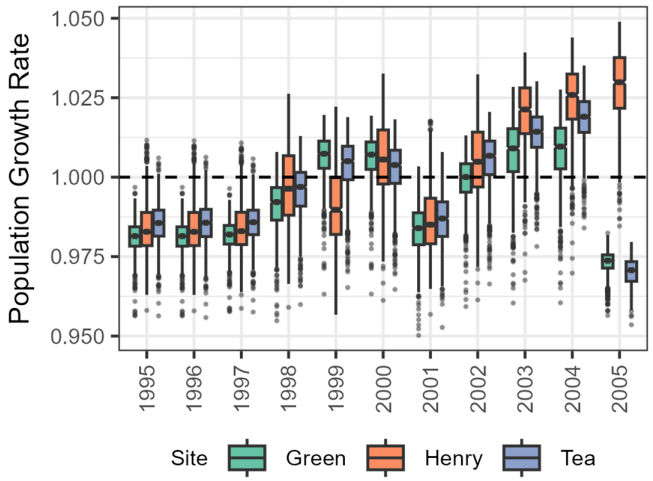

FIGURE 9 Population growth simulated during the questing season each year for the Weather and Mice (4) model at the three Cary field sites. The horizontal dashed line represents the threshold value of 1 (above the population is growing, below declining). Box plots were drawn with 2000 simulations. The lower and upper bounds of the box represent the 25% and 75% percentiles, respectively. The central line within the box represents the median. The whiskers extend to show the 95% CI, and the points outside the whiskers represent simulations outside the 95% CI.

the model is set to zero), which is consistent with the seasonal dormancy of nymphs in the northeastern United States. After this period, newly molted nymphs begin questing, and the model allows for the onset of questing nymphs by allowing transition to occur according to CGDDs (transition in the model is set to one). Defining the nymph questing season in this way caused nymphs to "emerge" as a single cohort, which is more representative of their actual questing behavior (Ogden et al., 2018), and suggests that adding the overwintering stage pushed the model to a more ecologically relevant structure. This is further demonstrated by the severe reduction in process error (i.e., model structural error) for nymphs in the four-stage models compared with the three-stage model.

Variance partitioning

In terms of improving tick predictions, an important conclusion of the variance partitioning is that the major obstacle to constraining predictions of peak tick abundance is uncertainty in the initial state. The IC uncertainty reflects the precision (or lack thereof) in knowing how many questing ticks, of any life stage, there are when making a new forecast, and was the dominant source of uncertainty during the nymph questing season. This has important implications for large-scale monitoring programs, such as the National Ecological Observatory Network (NEON), that have to make budgetary decisions about when and where to sample (Springer et al., 2016). We show that for reducing uncertainty in nymph predictions, the most important life stage for understanding transmission of tick-borne pathogens, sampling efforts should be directed toward monitoring during the period when nymphs are most active. Our modeling framework could be used to run Observing System Simulation Experiments to determine how to deploy field monitoring more effectively, quantify the value of information for different sampling periods, and evaluate whether iterative population forecasts could be used in an adaptive monitoring framework to optimize field sampling design.

The variance partitioning analysis shows interesting trends in both total and relative variance. For all life stages, total predictive variance tends to increase during the questing period. This was expected, as abundances are low or zero during nonquesting periods and thus have little variance. Likewise, during these nonquesting periods, most of the variance is comprised of process error because transition parameters are set to zero. Interestingly, the relative contribution of process error generally decreased during questing periods. This was due to the rapid increase of IC uncertainty when questing begins (Figure 8). In contrast to the dominance of IC uncertainty, the minimal contribution of parameter error suggests that the model could accommodate additional complexity; however, the limited contribution of process error during the questing season and the limited overall uncertainty in the dormant season when process error dominates suggest there may be limited returns to such an investment.

Mouse population models

The mouse population submodel was able to accurately estimate mouse abundance and constrained the daily survival rate of *P. leucopus* with temperature and precipitation on a daily basis. Our survival rates are slightly higher than those previously estimated; our monthly survival rates of 0.8 (converted from the daily rate) are higher than Collins and Kays (2014), which estimated a monthly rate of 0.5, and our 6-month rate (0.27) was higher than Previtali et al. (2010), which estimated a 6-month survival rate of *P. maniculatus* at 0.13. We attribute our higher survival estimate to the length of our study, 11 years, which allowed for recapturing mice over multiple seasons. Of course, real differences between sites in survival rates could have occurred based on, for example, different predator guilds, resource abundances, and abiotic regimes. Furthermore, we drove the temporal change in survival with temperature and precipitation,

and, to our knowledge, this is the first study to use such a fine temporal scale of abiotic variables to drive a mouse demographic model. Past studies have aggregated weather to monthly or seasonal intervals (Dhawan et al., 2018; Lewellen & Vessey, 1998; Previtali et al., 2010). Our results of daily precipitation and temperature reducing daily survival provide support for Lewellen and Vessey's (1998) result that summer drought reduces the weekly rate of population growth, and Dhawan et al.'s (2018) result that temperature negatively affects monthly population growth. We argue that our finer temporal scale accurately reflects demographic change as the effects of weather can be instantaneous as well as delayed and that there is little prior basis for selecting a timescale at which to aggregate.

Population growth rate

We found that over the 11 years of this study, the growth rate of the tick populations at the Cary Institute was variable but trended toward increasing abundance. Furthermore, we showed that population growth is most sensitive to the survival of nymphs and adults and less sensitive to the survival of larvae (Figure 9; Appendix S1: Figure S6). A key advance in our approach is that we modeled survival and transition across life stages within the daily transition matrix fit with field data. Additionally, our model incorporated the effect of host abundance, which we believe contributed to model transferability across sites, because they are an additional measure of seasonality and are directly responsible for moving ticks from one life stage to the next.

CONCLUSION

Our primary objective was to build a flexible and generalizable model that was fit and validated in a specific region with some of the most comprehensive tick population data available. We show that a generalized matrix model structure that reflects the complex life history of ticks was able to predict observations of larvae (Appendix S1: Figure S9) and nymphs (Figure 7). The modeling approach incorporates abiotic and biotic drivers independently at multiple life stages and allowed for a population growth estimate. The addition of an overwintering latent state was supported by the dramatic reduction in model process error. Furthermore, the variance partitioning analysis showed that our ability to predict nymph abundance during the questing season is most limited by low-latency nymph monitoring data, which are needed to constrain model initial conditions. We expect that the modeling approach and results herein will be transferable to other locations and times, because both the model and data are not overly complex (Yates et al., 2018) and comparable data on ticks, hosts, and climate are broadly available (Springer et al., 2016). We recommend future work focus on improving data to support modeling the adult stage by exploring different drivers for survival, incorporating reproductive hosts in the fecundity parameter, or adding a latent state between questing nymphs and questing adults. As Lyme disease has more than doubled in the past decade (CDC, 2021), a more predictive understanding is needed to quantify Lyme disease risk (Kilpatrick et al., 2017), and our quantitative predictions for nymph abundance move the field forward in this regard (Ostfeld et al., 2006).

AUTHOR CONTRIBUTIONS

John R. Foster led the model development with oversight from Shannon L. LaDeau, Richard S. Ostfeld, and Michael C. Dietze. Kelly Oggenfuss facilitated and directed data management. Funding for the modeling effort was procured by Shannon L. LaDeau and Michael C. Dietze, with funding for fieldwork procured by Richard S. Ostfeld. The first draft of the manuscript was written by John R. Foster; all drafts thereafter were edited and revised by all the authors.

ACKNOWLEDGMENTS

We thank the many field biologists at the Cary Institute of Ecosystem Studies for collecting the field data used in this study. Additionally, Cary staff who facilitated collaboration and data management include Deb Fargione, Cassandra Harrison, and Amy Schuler. We thank Peter Buston, Anne Short Gianotti, Charlotte Malmborg, Tess McCabe, Kathryn Wheeler, Zoey Werbin, and Katie Zarada for their feedback on early drafts of this manuscript. Funding was provided by the National Science Foundation, most recently grant DEB1947756.

CONFLICT OF INTEREST STATEMENT

The authors declare no conflicts of interest.

DATA AVAILABILITY STATEMENT

Tick survival data (Brunner et al., 2022) are available from Dryad: https://doi.org/10.5061/dryad.931zcrjnz. Tick and mouse data (Ostfeld & Oggenfuss, 2023) are available from the Cary Institute of Ecosystem Studies via Figshare: https://doi.org/10.25390/caryinstitute.23611374.v1. Code (Foster, 2023) is available from Zenodo: https://doi.org/10.5281/zenodo.8097453.

ORCID

John R. Foster https://orcid.org/0000-0002-7526-3177
Michael C. Dietze https://orcid.org/0000-0002-2324-2518

REFERENCES

Barbour, A. G., and D. Fish. 1993. "The Biological and Social Phenomenon of Lyme Disease." *Science, New Series* 260(5114): 1610–16.

Berger, K. A., H. S. Ginsberg, L. Gonzalez, and T. N. Mather. 2014. "Relative Humidity and Activity Patterns of *Ixodes scapularis* (Acari: Ixodidae)." *Journal of Medical Entomology* 51(4): 769–776. https://doi.org/10.1603/ME13186.

Brooks, S. P., and A. Gelman. 1998. "General Methods for Monitoring Convergence of Iterative Simulations." *Journal of Computational and Graphical Statistics* 7(4): 434–455. https://doi.org/10.1080/10618600.1998.10474787.

Brunner, J. L., M. Killilea, and R. S. Ostfeld. 2012. "Overwintering Survival of Nymphal *Ixodes scapularis* (Acari: Ixodidae) under Natural Conditions." *Journal of Medical Entomology* 49(5): 981–87. https://doi.org/10.1603/ME12060.

Brunner, J. L., S. L. LaDeau, M. Killelea, E. Valentine, M. Schierer, and R. S. Ostfeld. 2023. "Off-Host Survival of Blacklegged Ticks in Eastern North America: A Multistage, Multiyear, Multisite Study." *Ecological Monographs* 93(3): e1572. https://doi.org/10.1002/ecm.1572.

Brunner, J. L., and R. S. Ostfeld. 2008. "Multiple Causes of Variable Tick Burdens on Small-Mammal Hosts." *Ecology* 89(8): 2259–72. https://doi.org/10.1890/07-0665.1.

Brunner, J., R. Ostfeld, S. LaDeau, E. Valentine, M. Schierer, and M. Killilea. 2022. "Data For: Off-Host Survival of Blacklegged Ticks in Eastern North America: A Multi-Stage, Multi-Year, and Multi-Site Study [Dataset]." Dryad. https://doi.org/10.5061/dryad.931zcrjnz.

Caswell, H. 2000. *Matrix Population Models*, Vol. 1. Sunderland, MA: Sinauer Sunderland.

CDC. 2021. "Lyme Disease Charts and Figures: Historical Data|Lyme Disease." CDC. https://www.cdc.gov/lyme/stats/graphs.html.

Collins, C. R., and R. W. Kays. 2014. "Patterns of Mortality in a Wild Population of White-Footed Mice." *Northeastern Naturalist* 21(2): 323–336. https://doi.org/10.1656/045.021.0213.

de Valpine, P., C. Paciorek, D. Turek, N. Michaud, C. Anderson-Bergman, F. Obermeyer, C. W. Cortes, A. Rodrìguez, D. T. Lang, and S. Paganin. 2022. "NIMBLE: MCMC, Particle Filtering, and Programmable Hierarchical Modeling (version 0.12.2)." https://doi.org/10.5281/zenodo.1211190.

Dhawan, R., I. R. Fischhoff, and R. S. Ostfeld. 2018. "Effects of Weather Variability on Population Dynamics of White-Footed Mice (*Peromyscus leucopus*) and Eastern Chipmunks (*Tamias striatus*)." *Journal of Mammalogy* 99(6): 1436–43. https://doi.org/10.1093/jmammal/gyy126.

Dietze, M. 2017a. *Ecological Forecasting*. Princeton University Press. https://doi.org/10.2307/j.ctvc7796h.

Dietze, M. C. 2017b. "Prediction in Ecology: A First-Principles Framework." *Ecological Applications* 27(7): 2048–60. https://doi.org/10.1002/eap.1589.

Dobson, A. D. M., T. J. R. Finnie, and S. E. Randolph. 2011. "A Modified Matrix Model to Describe the Seasonal Population Ecology of the European Tick *Ixodes ricinus*: *Ixodes ricinus* Population Model." *Journal of Applied Ecology* 48(4): 1017–28. https://doi.org/10.1111/j.1365-2664.2011.02003.x.

Eisen, R. J., L. Eisen, C. B. Graham, A. Hojgaard, P. S. Mead, G. Kersch, S. Karpathy, et al. 2019. *Surveillance for Ixodes scapularis and Pathogens Found in this Tick Species in the United States*, Vol. 1, 34. Centers for Disease Control and Prevention. https://www.cdc.gov/ticks/resources/TickSurveillance_Iscapularis-P.pdf

Eisen, R. J., and L. Eisen. 2018. "The Blacklegged Tick, *Ixodes scapularis*: An Increasing Public Health Concern." *Trends in Parasitology* 34(4): 295–309. https://doi.org/10.1016/j.pt.2017.12.006.

Evans, M. E. K., K. E. Holsinger, and E. S. Menges. 2010. "Fire, Vital Rates, and Population Viability: A Hierarchical Bayesian Analysis of the Endangered Florida Scrub Mint." *Ecological Monographs* 80(4): 627–649. https://doi.org/10.1890/09-1758.1.

Foster, J. 2023. "JohnRFoster/matrix_model_ixodes: Matrix Model (v1.0.0)." Zenodo. https://doi.org/10.5281/zenodo.8097453.

Gelman, A., and D. B. Rubin. 1992. "Inference from Iterative Simulation Using Multiple Sequences." *Statistical Science* 7(4): 457–472. https://doi.org/10.1214/ss/1177011136.

Gestel, V., E. M. Mats, D. Heylen, and K. Verheyen. 2022. "Survival in the Understorey: Testing Direct and Indirect Effects of Microclimatological Changes on *Ixodes ricinus*." *Ticks and Tick-borne Diseases* 13(6): 102035. https://doi.org/10.1016/j.ttbdis.2022.102035.

Ginsberg, H. S., M. Albert, L. Acevedo, M. C. Dyer, I. M. Arsnoe, J. I. Tsao, T. N. Mather, and R. A. LeBrun. 2017. "Environmental Factors Affecting Survival of Immature *Ixodes scapularis* and Implications for Geographical Distribution of Lyme Disease: The Climate/Behavior Hypothesis." *PLoS One* 12(1): e0168723. https://doi.org/10.1371/journal.pone.0168723.

Ginsberg, H. S., E. L. Rulison, A. Azevedo, G. C. Pang, I. M. Kuczaj, J. I. Tsao, and R. A. LeBrun. 2014. "Comparison of Survival Patterns of Northern and Southern Genotypes of the North American Tick *Ixodes scapularis* (Acari: Ixodidae) under Northern and Southern Conditions." *Parasites & Vectors* 7(1): 394. https://doi.org/10.1186/1756-3305-7-394.

Gneiting, T., and A. E. Raftery. 2007. "Strictly Proper Scoring Rules, Prediction, and Estimation." *Journal of the American Statistical Association* 102(477): 359–378. https://doi.org/10.1198/016214506000001437.

Gray, J., O. Kahl, R. S. Lane, and G. Stanek. 2002. *Lyme Borreliosis: Biology, Epidemiology, and Control*. Wallingford: CABI.

Gross, K., B. A. Craig, and W. D. Hutchison. 2002. "Bayesian Estimation of a Demographic Matrix Model from Stage-Frequency Data." *Ecology* 83(12): 3285–98.

Hayes, L. E., J. A. Scott, and K. C. Stafford. 2015. "Influences of Weather on *Ixodes scapularis* Nymphal Densities at Long-Term Study Sites in Connecticut." *Ticks and Tick-borne Diseases* 6(3): 258–266. https://doi.org/10.1016/j.ttbdis.2015.01.006.

Hooten, M. B., and N. T. Hobbs. 2015. "A Guide to Bayesian Model Selection for Ecologists." *Ecological Monographs* 85(1): 3–28. https://doi.org/10.1890/14-0661.1.

Jolly, G. M. 1965. "Explicit Estimates from Capture-Recapture Data with Both Death and Immigration-Stochastic Model." *Biometrika* 52(1/2): 225–247.

Jones, C. J., and U. D. Kitron. 2000. "Populations of *Ixodes scapularis* (Acari: Ixodidae) Are Modulated by Drought at a Lyme Disease Focus in Illinois." *Journal of Medical Entomology* 37(3): 8–415.

Keesing, F., J. Brunner, S. Duerr, M. Killilea, K. LoGiudice, K. Schmidt, H. Vuong, and R. S. Ostfeld. 2009. "Hosts as

Ecological Traps for the Vector of Lyme Disease." *Proceedings of the Royal Society B: Biological Sciences* 276(1675): 3911–19. https://doi.org/10.1098/rspb.2009.1159.

Kelly, V. 2020. *Cary Environmental Monitoring Program Daily Meteorological and Solar Radiation Data: 1988-2021*. Millbrook, New York: Cary Institute. https://doi.org/10.25390/caryinstitute.11553219.v3.

Kéry, M., and M. Schaub. 2011. "Estimation of Survival, Recruitment, and Population Size from Capture–Recapture Data Using the Jolly–Seber Model." In *Bayesian Population Analysis Using WinBUGS: A Hierarchical Perspective. First*, edited by Kéry, M., and M. Schaub, 316–346. Waltham: Elsevier. https://doi.org/10.1016/B978-0-12-387020-9.00010-9.

Kessler, W. H., C. Ganser, and G. E. Glass. 2019. "Modeling the Distribution of Medically Important Tick Species in Florida." *Insects* 10(7): 190. https://doi.org/10.3390/insects10070190.

Kilpatrick, A. M., A. D. M. Dobson, T. Levi, D. J. Salkeld, A. Swei, H. S. Ginsberg, A. Kjemtrup, et al. 2017. "Lyme Disease Ecology in a Changing World: Consensus, Uncertainty and Critical Gaps for Improving Control." *Philosophical Transactions of the Royal Society B: Biological Sciences* 372 (1722): 20160177. https://doi.org/10.1098/rstb.2016.0117.

LaDeau, S. L., G. E. Glass, N. Thompson Hobbs, A. Latimer, and R. S. Ostfeld. 2011. "Data–Model Fusion to Better Understand Emerging Pathogens and Improve Infectious Disease Forecasting." *Ecological Applications* 21(5): 1443–60. https://doi.org/10.1890/09-1409.1.

Levi, T., F. Keesing, K. Oggenfuss, and R. S. Ostfeld. 2015. "Accelerated Phenology of Blacklegged Ticks under Climate Warming." *Philosophical Transactions of the Royal Society B: Biological Sciences* 370(1665): 20130556. https://doi.org/10.1098/rstb.2013.0556.

Levi, T., Keesing, F., Holt, R. D., Barfield, M., and Ostfeld, R. S. 2016. Quantifying Dilution and Amplification in a Community of Hosts for Tick-Borne Pathogens. *Ecological Applications*, 26 (2): 484–498.

Lewellen, R. H., and S. H. Vessey. 1998. "The Effect of Density Dependence and Weather on Population Size of a Polyvoltine Species." *Ecological Monographs* 68(4): 571–594. https://doi.org/10.1890/0012-9615(1998)068[0571:TEODDA]2.0.CO;2.

Lindsay, L. R., I. K. Barker, G. A. Surgeoner, S. A. Mcewen, T. J. Gillespie, and E. M. Addison. 1998. "Survival and Development of the Different Life Stages of *Ixodes scapularis* (Acari: Ixodidae) Held within Four Habitats on Long Point, Ontario, Canada." *Journal of Medical Entomology* 35(3): 189–199. https://doi.org/10.1093/jmedent/35.3.189.

Mather, T. N., M. C. Nicholson, E. F. Donnelly, and B. T. Matyas. 1996. "Entomologic Index for Human Risk of Lyme Disease." *American Journal of Epidemiology* 144(11): 1066–69. https://doi.org/10.1093/oxfordjournals.aje.a008879.

Merritt, J. F., M. Lima, and F. Bozinovic. 2001. "Seasonal Regulation in Fluctuating Small Mammal Populations: Feedback Structure and Climate." *Oikos* 94(3): 505–514. https://doi.org/10.1034/j.1600-0706.2001.940312.x.

Michielsens, C. G. J., M. K. McAllister, S. Kuikka, S. Mäntyniemi, A. Romakkaniemi, T. Pakarinen, L. Karlsson, and L. Uusitalo. 2008. "Combining Multiple Bayesian Data Analyses in a Sequential Framework for Quantitative Fisheries Stock Assessment." *Canadian Journal of Fisheries and Aquatic Sciences* 65(5): 962–974. https://doi.org/10.1139/f08-015.

Needham, G. R. 1991. "Off-Host Physiological Ecology of Ixodid Ticks." *Annual Review of Entomology* 36: 659–681. https://doi.org/10.1146/annurev.en.36.010191.003303.

Nicholson, M. C., and T. N. Mather. 1996. "Methods for Evaluating Lyme Disease Risks Using Geographic Information Systems and Geospatial Analysis." *Journal of Medical Entomology* 33(5): 711–720. https://doi.org/10.1093/jmedent/33.5.711.

Ogden, N. H., M. Bigras-Poulin, K. Hanincová, A. Maarouf, C. J. O'Callaghan, and K. Kurtenbach. 2008. "Projected Effects of Climate Change on Tick Phenology and Fitness of Pathogens Transmitted by the North American Tick *Ixodes scapularis*." *Journal of Theoretical Biology* 254(3): 621–632. https://doi.org/10.1016/j.jtbi.2008.06.020.

Ogden, N. H., M. Bigras-Poulin, C. J. O'Callaghan, I. K. Barker, L. R. Lindsay, A. Maarouf, K. E. Smoyer-Tomic, D. Waltner-Toews, and D. Charron. 2005. "A Dynamic Population Model to Investigate Effects of Climate on Geographic Range and Seasonality of the Tick *Ixodes scapularis*." *International Journal for Parasitology* 35(4): 375–389. https://doi.org/10.1016/j.ijpara.2004.12.013.

Ogden, N. H., G. Pang, H. S. Ginsberg, G. J. Hickling, R. L. Burke, L. Beati, and J. I. Tsao. 2018. "Evidence for Geographic Variation in Life-Cycle Processes Affecting Phenology of the Lyme Disease Vector *Ixodes scapularis* (Acari: Ixodidae) in the United States." *Journal of Medical Entomology* 55(6): 1386–1401. https://doi.org/10.1093/jme/tjy104.

Ogden, N. H., M. Radojevic, X. Wu, V. R. Duvvuri, P. A. Leighton, and J. Wu. 2014. "Estimated Effects of Projected Climate Change on the Basic Reproductive Number of the Lyme Disease Vector *Ixodes scapularis*." *Environmental Health Perspectives* 122(6): 631–38. https://doi.org/10.1289/ehp.1307799.

Ostfeld, R. 2011. *Lyme Disease: The Ecology of a Complex System*. New York: OUP USA.

Ostfeld, R., and K. Oggenfuss. 2023. "Long Term Monitoring of the Dynamics of Rodents, Ticks and Lyme Disease Risk in Oak Forests: Mouse and Tick Data, 1995–2005." Figshare. Dataset. https://doi.org/10.25390/caryinstitute.23611374.v1.

Ostfeld, R. S., and J. L. Brunner. 2015. "Climate Change and *Ixodes* Tick-Borne Diseases of Humans." *Philosophical Transactions of the Royal Society B: Biological Sciences* 370(1665): 20140051. https://doi.org/10.1098/rstb.2014.0051.

Ostfeld, R. S., C. D. Canham, K. Oggenfuss, R. J. Winchcombe, and F. Keesing. 2006. "Climate, Deer, Rodents, and Acorns as Determinants of Variation in Lyme-Disease Risk." *PLoS Biology* 4(6): e145. https://doi.org/10.1371/journal.pbio.0040145.

Ostfeld, R. S., C. G. Jones, and J. O. Wolff. 1996. "Of Mice and Mast." *BioScience* 46(5): 323–330. https://doi.org/10.2307/1312946.

Ostfeld, R. S., T. Levi, F. Keesing, K. Oggenfuss, and C. D. Canham. 2018. "Tick-Borne Disease Risk in a Forest Food Web." *Ecology* 99(7): 1562–73. https://doi.org/10.1002/ecy.2386.

Ostfeld, R. S., E. M. Schauber, C. D. Canham, F. Keesing, C. G. Jones, and J. O. Wolff. 2001. "Effects of Acorn Production and Mouse Abundance on Abundance and *Borrelia burgdorferi* Infection Prevalence of Nymphal *Ixodes scapularis* Ticks."

Vector-Borne and Zoonotic Diseases 1(1): 55–63. https://doi.org/10.1089/153036601750137688.

Pepin, K. M., R. J. Eisen, P. S. Mead, J. Piesman, D. Fish, A. G. Hoen, A. G. Barbour, S. Hamer, and M. A. Diuk-Wasser. 2012. "Geographic Variation in the Relationship between Human Lyme Disease Incidence and Density of Infected Host-Seeking *Ixodes scapularis* Nymphs in the Eastern United States." *The American Journal of Tropical Medicine and Hygiene* 86(6): 1062–71. https://doi.org/10.4269/ajtmh.2012.11-0630.

Perret, J.-L., O. Rais, and L. Gern. 2004. "Influence of Climate on the Proportion of *Ixodes ricinus* Nymphs and Adults Questing in a Tick Population." *Journal of Medical Entomology* 41(3): 361–65. https://doi.org/10.1603/0022-2585-41.3.361.

Piesman, J., G. O. Maupin, E. G. Campos, and C. M. Happ. 1991. "Duration of Adult Female *Ixodes dammini* Attachment and Transmission of *Borrelia burgdorferi*, with Description of a Needle Aspiration Isolation Method." *The Journal of Infectious Diseases* 163(4): 895–97. https://doi.org/10.1093/infdis/163.4.895.

Plummer, M., N. Best, K. Cowles, and K. Vines. 2006. "CODA: Convergence Diagnosis and Output Analysis for MCMC." *R News* 6(1): 7–11.

Plummer, M. 2003. "JAGS: A Program for Analysis of Bayesian Graphical Models Using Gibbs Sampling." In *Proceedings of the 3rd International Workshop on Distributed Statistical Computing*, 124, 1–10. Vienna.

Previtali, M. A., E. M. Lehmer, J. M. C. Pearce-Duvet, J. D. Jones, C. A. Clay, B. A. Wood, P. W. Ely, S. M. Laverty, and M. D. Dearing. 2010. "Roles of Human Disturbance, Precipitation, and a Pathogen on the Survival and Reproductive Probabilities of Deer Mice." *Ecology* 91(2): 582–592. https://doi.org/10.1890/08-2308.1.

R Core Team. 2020. *R: A Language and Environment for Statistical Computing*. Vienna: R Foundation for Statistical Computing. https://www.R-project.org/.

Richter, D., A. Debski, Z. Hubalek, and F.-R. Matuschka. 2012. "Absence of Lyme Disease Spirochetes in Larval *Ixodes ricinus* Ticks." *Vector-Borne and Zoonotic Diseases* 12(1): 21–27. https://doi.org/10.1089/vbz.2011.0668.

Rollend, L., D. Fish, and J. E. Childs. 2013. "Transovarial Transmission of *Borrelia spirochetes* by *Ixodes scapularis*: A Summary of the Literature and Recent Observations." *Ticks and Tick-borne Diseases* 4(1): 46–51. https://doi.org/10.1016/j.ttbdis.2012.06.008.

Royle, J. A. 2004. "N-Mixture Models for Estimating Population Size from Spatially Replicated Counts." *Biometrics* 60(1): 108–115. https://doi.org/10.1111/j.0006-341X.2004.00142.x.

Schauber, E. M., R. S. Ostfeld, and A. S. Evans. 2005. "What Is the Best Predictor of Annual Lyme Disease Incidence: Weather, Mice, or Acorns?" *Ecological Applications* 15(2): 575–586. https://doi.org/10.1890/03-5370.

Schmidt, K. A., and R. S. Ostfeld. 2001. "Biodiversity and the Dilution Effect in Disease Ecology." *Ecology* 82(3): 609–619. https://doi.org/10.1890/0012-9658(2001)082[0609:BATDEI]2.0.CO;2.

Seber, G. A. F. 1965. "A Note on the Multiple-Recapture Census." *Biometrika* 52(1/2): 249–259.

Simonis, J. L., E. P. White, and S. K. Morgan Ernest. 2021. "Evaluating Probabilistic Ecological Forecasts." *Ecology* 102(8): e03431. https://doi.org/10.1002/ecy.3431.

Sonenshine, D. 2018. "Range Expansion of Tick Disease Vectors in North America: Implications for Spread of Tick-Borne Disease." *International Journal of Environmental Research and Public Health* 15(3): 478. https://doi.org/10.3390/ijerph15030478.

Springer, Y. P., D. Hoekman, P. T. J. Johnson, P. A. Duffy, R. A. Hufft, D. T. Barnett, B. F. Allan, et al. 2016. "Tick-, Mosquito-, and Rodent-Borne Parasite Sampling Designs for the National Ecological Observatory Network." *Ecosphere* 7(5): e01271. https://doi.org/10.1002/ecs2.1271.

Stafford, K. C., M. L. Cartter, L. A. Magnarelli, S.-H. Ertel, and P. A. Mshar. 1998. "Temporal Correlations between Tick Abundance and Prevalence of Ticks Infected with *Borrelia burgdorferi* and Increasing Incidence of Lyme Disease." *Journal of Clinical Microbiology* 36(5): 1240–44. https://doi.org/10.1128/JCM.36.5.1240-1244.1998.

Stanek, G., G. P. Wormser, J. Gray, and F. Strle. 2012. "Lyme Borreliosis." *The Lancet* 379(9814): 461–473. https://doi.org/10.1016/S0140-6736(11)60103-7.

Tredennick, A. T., M. B. Hooten, and P. B. Adler. 2017. "Do We Need Demographic Data to Forecast Plant Population Dynamics?" *Methods in Ecology and Evolution* 8(5): 541–551. https://doi.org/10.1111/2041-210X.12686.

Valpine, P. D., D. Turek, C. J. Paciorek, C. Anderson-Bergman, D. T. Lang, and R. Bodik. 2017. "Programming with Models: Writing Statistical Algorithms for General Model Structures with NIMBLE." *Journal of Computational and Graphical Statistics* 26(2): 403–413. https://doi.org/10.1080/10618600.2016.1172487.

Wang, G., J. O. Wolff, S. H. Vessey, N. A. Slade, J. W. Witham, J. F. Merritt, M. L. Hunter, and S. P. Elias. 2009. "Comparative Population Dynamics of *Peromyscus leucopus* in North America: Influences of Climate, Food, and Density Dependence." *Population Ecology* 51(1): 133–142. https://doi.org/10.1007/s10144-008-0094-4.

Wilson, M. L., T. S. Litwin, T. A. Gavin, M. C. Capkanis, D. C. Maclean, and A. Spielman. 1990. "Host-Dependent Differences in Feeding and Reproduction of *Ixodes dammini* (Acari: Ixodidae)." *Journal of Medical Entomology* 27(6): 945–954. https://doi.org/10.1093/jmedent/27.6.945.

Yates, K. L., P. J. Bouchet, M. Julian Caley, K. Mengersen, C. F. Randin, S. Parnell, A. H. Fielding, et al. 2018. "Outstanding Challenges in the Transferability of Ecological Models." *Trends in Ecology & Evolution* 33(10): 790–802. https://doi.org/10.1016/j.tree.2018.08.001.

SUPPORTING INFORMATION

Additional supporting information can be found online in the Supporting Information section at the end of this article.

How to cite this article: Foster, John R., Shannon L. LaDeau, Kelly Oggenfuss, Richard S. Ostfeld, and Michael C. Dietze. 2024. "A Modified Matrix Model Captures the Population Dynamics for the Primary Vector of Lyme Disease in North America." *Ecosphere* 15(10): e70022. https://doi.org/10.1002/ecs2.70022